NASA-CR-196026

DEVELOPMENT OF POINTS AS A PLANETOLOGY INSTRUMENT

IN72-CR
IN-91-CR
12626
27P

NASA Grant NAGW-2497

Annual Performance Report

For the period 1 October 1993 through 30 September 1994

Principal Investigator

Dr. Robert D. Reasenberg

May 1994

N94-35265
Unclas
G3/91 0012620

Prepared for
National Aeronautics and Space Administration
Washington, DC 20546

Smithsonian Institution
Astrophysical Observatory
Cambridge, Massachusetts 02138

(NASA-CR-196026) DEVELOPMENT OF POINTS AS A PLANETOLOGY INSTRUMENT Annual Report No. 5, 1 Oct. 1993 - 30 Sep. 1994 (Smithsonian Astrophysical Observatory) 27 p

The Smithsonian Astrophysical Observatory
is a member of the
Harvard-Smithsonian Center for Astrophysics

Annual Performance Report No. 5

Development Of Points As A Planetology Instrument

During the reporting period, we carried out investigations required to enhance our design of POINTS as a tool for the search for and characterization of extra-solar planetary systems. The results of that work was included in a paper on POINTS as well as one on Newcomb, which will soon appear in the proceedings of SPIE Conference 2200. (Newcomb is a spinoff of POINTS. It is a small astrometric interferometer now being developed jointly by SAO and the US Navy. It could help establish some of the technology needed for POINTS.) These papers are appended.

POINTS: an astrometric spacecraft with multifarious applications

R.D. Reasenberg, R.W. Babcock, M.A. Murison, M.C. Noecker, J.D. Phillips

Smithsonian Astrophysical Observatory
Harvard-Smithsonian Center for Astrophysics
60 Garden Street, Cambridge, MA 02138

B.L. Schumaker, J.S. Ulvestad

Jet Propulsion Laboratory
4800 Oak Grove Drive
Pasadena, CA 91109

ABSTRACT

POINTS is a dual astrometric optical interferometer with nominal baseline length of 2 meters and measurement accuracy of 5 microarcseconds for targets separated by about 90 degrees on the sky. If selected as the ASEPS-1 mission, it could perform a definitive search for extra-solar planetary systems, either finding and characterizing a large number of them or showing that they are far less numerous than now believed. If selected as AIM, it could be a powerful new multidisciplinary research tool, opening new areas of astrophysical research and changing the nature of the questions being asked in some old areas. Based on a preliminary indication of the observational needs of the two missions, we find that a single POINTS mission lasting ten years would meet the science objectives of both ASEPS-1 and AIM. POINTS, which is small, agile, and mechanically simple, would be the first of a new class of powerful instruments in space and would prove the technology for the larger members of the class that are expected to follow. The instrument is designed around a metrology system that measures both the critical distances internal to the starlight interferometers and the angle between them. Rapid measurement leads to closure on the sky and the ability to detect and correct time-dependent measurement biases.

2. INTRODUCTION AND OVERVIEW

POINTS (Precision Optical INTerferometer in Space) is an Earth-orbiting astrometric instrument designed to measure the angle between a pair of stars, separated by about 90 deg, with a nominal accuracy of 5 microarcseconds (μas). See Fig. 1. POINTS will provide a powerful new multi-disciplinary tool for astronomical research. It comprises a pair of independent Michelson stellar interferometers and a metrology system based on laser gauges. The wide target separation leads to global astrometry, which was first possible with HIPPARCOS[1]. That wide separation yields three principal advantages: (1) The astrometric data contain 360 deg closure information for calibrating the measurements; (2) There are always numerous bright reference stars available for a selected target star; and (3) Parallax measurements are absolute and can be made for targets that lack suitable nearby references.

The success of the HIPPARCOS mission and the strong efforts now being made within the European space community to start a follow-on astrometric mission (e.g., Roemer[2] and GAIA[3]) attest to the scientific richness of modern, spaceborne astrometry. A series of astrometric measurements of a target yield its position and (possibly complex) motion. For high precision astrometry, the position is of little interest unless it can be compared to an alternative position measurement, for example, at a substantially different wavelength. Measured motion can provide a variety of results. (1) Annual periodic motion yields parallax, arguably the most important astrometric determination for astrophysics. (2) Other periodic motion implies one or more companions. (3) Linear motion of a related group of objects implies a flow, such as may be associated with the process that forms spiral arms in the Galaxy or with cluster membership. Finally, (4) special signatures are associated with gravitational lensing and (the closely related) deflection test of general relativity[4,5,6].

POINTS is a candidate for two NASA missions under the Office of Space Science (OSS). Within the Solar System Exploration Division of OSS, the Planetary System Science Program includes the Astronomical Search for Extra-solar Planetary Systems (ASEPS). The first spacebased component, the ASEPS-1 mission (previously called TOPS-1),

would be required to search to sufficient depth that a negative result would be scientifically significant[7]. Designed to fulfill generously the science objectives of the ASEPS-1 program, POINTS can accomplish a definitive search for extra-solar planetary systems by monitoring more than 1500 stars for a decade to detect the motion around the star-planet barycenter. It would either find and characterize a large number of planetary systems or show that they are far less numerous than now believed. Within the Astrophysics Division of OSS, consideration is being given to the Astrometric Interferometry Mission (AIM) as recommended by the Bahcall Committee[8]. AIM would address a wide variety of astrophysical questions ranging from the Cepheid distance scale to the mass of the Galaxy [9,10]. Particularly because of its capability for determining parallax, POINTS would open new areas of astrophysical research and change the nature of the questions being asked in some old areas. Based on a preliminary indication of the observational needs of the two missions, we find that a single POINTS mission lasting ten years would meet the science objectives of both ASEPS-1 and AIM without using all of the available observing time. Of course, either mission could be expanded to use all of the capacity of any reasonable instrument proposed.

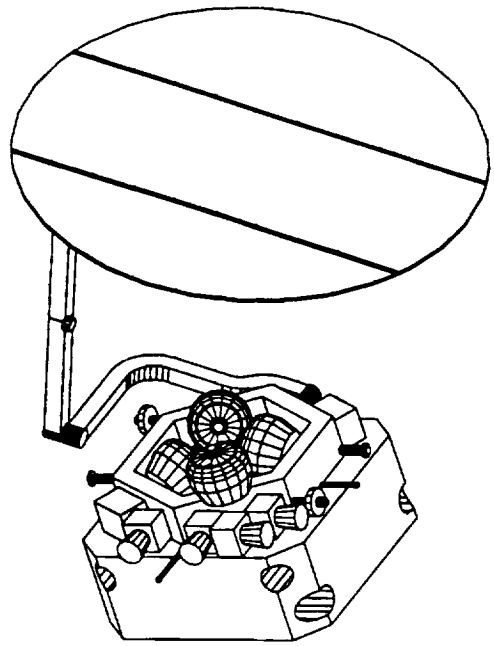

Figure 1. The POINTS spacecraft configured for astrometric observation. (D. Noon, JPL) The instrument and bus are in the shadow of the 4.8 meter diameter solar shield.

The nominal orbit for POINTS, which is circular at 100,000 km from Earth, provides access to most of the sky, a steady thermal environment, substantially reduced gravity gradient torque and occultation time compared to low Earth orbit, and easy access to ground facilities for communications and tracking. The instrument detects a dispersed fringe (channelled spectrum) and therefore can both tolerate large pointing errors and preserve information about compound targets for future analysis, *i.e.*, when the point-like assumption needs to be re-examined. In operation, the difficult problem of measuring the angular separation of widely spaced star pairs is reduced to two less difficult problems: that of measuring the angle between the two stellar interferometers and that of measuring interferometrically the small offset of each star from the corresponding interferometer axis.

The mitigation of systematic error is the central theme of the instrument architecture and the data-analysis methods. Stable materials, precise thermal control, and continuous precise metrology are fundamental to the design of the instrument. A preliminary version of the required picometer laser metrology has been demonstrated in the laboratory to the level required for the flight instrument. Post-measurement detection and correction of time-dependent bias are the essential elements in data analysis. In that post-measurement analysis, individual measurements of star-pair separations are combined to determine both the coordinates (relative positions, absolute parallaxes, and proper motions) of all observed stars and several instrument parameters including overall time-dependent measurement bias. The resulting stellar coordinate estimates are both global and bias-free at the level of the uncertainty in the reduced (*i.e.*, combined and analyzed) measurements. Table 1 contains the principal parameters of the POINTS instrument.

There are four central issues that must be addressed for POINTS or any similar instrument. First, what is the measurement accuracy and the closely related scientific "throughput" $\Im = N/\sigma^2$? Here N is the number of observations per day and σ^2 is the measurement variance. Second, is the spacecraft sufficiently agile to make the large number of measurements per day needed by an ASEPS-1 mission? This is clearly related to throughput, but it specifically addresses the rate of slew, damping of slew transients, and target acquisition. Third, how well does the instrument match the requirements of the scientific mission? This includes sky coverage, ability to measure parallax for astrophysical studies, and spacecraft life, which is closely related to cost and complexity. Fourth and last, there is the question of systematic error. This question is the most important of the four and is central to the architecture of POINTS.

Table 1. Principal Parameters of the POINTS Instrument

Class	Parameter	Value
Interferometer		
	Number of stellar interferometers	2
	Length of baselines	2 m
	Number of subapertures per interferometer	2
	Subaperture diameter	35 cm
	Subaperture central obscuration	15 cm
	Optical passband	0.25-0.9 μm
	Photon detection probability	15%
Spectrometer		
	Prism angle	35 deg
	Focal length of off-axis parabola	27 cm
	Nominal fringe count	5
	Length of detector array	512 pixels
Measurement		
	Nominal measurement uncertainty	5 μas
	Observation time for a pair of mag 10 stars	2 minutes
	Observation rate (during search for planetary systems)	350 obs/day

POINTS reaches its nominal measurement accuracy of 5 μas in about 2 min when observing a pair of mag 10 stars. The instrument includes two separate stellar interferometers that have their principal optical axes (nominal target directions) separated by φ, an angle that is adjustable from 87 to 93 deg. A single measurement determines the angular separation of a pair of target stars.

For a given target star, the reference star is chosen from among the "reference-grid" stars within a great-circle band of sky that has an area of 2160 square degrees (>5% of the sky). The reference grid is a set of (say 300) bright stars that are redundantly observed periodically (say 4 times per year) throughout the mission. The grid stars would be bright (say $m \leq 10$), and many would be of scientific interest. In the observable band, there would be about 80 stars as bright as (visual) mag 5; 1200 stars, mag 7.5; and 17,000 stars, mag 10. Of the stars within the great-circle band, about 15 would be members of the reference grid. Thus, the observation time is not dominated by the low photon rate of dim reference stars. Further, each reference star is also a carefully studied target star. Its motions are well modelled and our covariance studies show that they do not significantly corrupt the measurements of other stars.

Because of the redundancy of the star-grid observations, the intra-grid measurements can be analyzed to yield a rigid frame; the measurements serve to determine the separations of all pairs of grid stars, even those that could not have been simultaneously observed. Further, a small number of bright quasars would be redundantly observed to provide rotational stability for the grid frame by connecting it to the best candidate inertial reference. In the standard observing scenario, all POINTS measurements would include at least one grid star. To study a target (star, quasar, *etc.*) that is not in the grid, a set of measurements would be made of the target with respect to a small subset of the grid stars.

The nominal POINTS observing schedule for the ASEPS-1 targets allows 4 min from the start of one observation to the start of the next. Of this, 1¼ min is slewing to and finding the next target pair, ¾ min is settling after slew and target fringe acquisition, and 2 min is observing. The slew time is based on the angular acceleration rate of the Attitude Control System (ACS) and a mean slew angle of 25 deg, which was found from a series of simulated annealing studies of scheduling for an ASEPS-1 mission.

3. INSTRUMENT DESCRIPTION AND CONCEPT

3.1. Principles of operation

The principal elements of the POINTS instrument are two starlight interferometers, mounted at a nearly right angle, and a metrology system. The instrument determines θ, the angular separation between two widely separated stars, by measuring φ, the angle between the interferometers, and measuring independently δ_1 and δ_2, the offsets of the target stars from their respective interferometer axes. With proper selection of target stars and a small adjustment capability in φ (nominally $87 \le \varphi \le 93$ deg), a pair of stars can be brought simultaneously near their respective interferometer axes. Once a target star is in the field of an interferometer, δ is measured through the analysis of the dispersed fringe, which forms a channelled spectrum. Central features of the instrument are the real-time monitoring of the angle between the interferometers and the metrology along the starlight optical path, each of which uses a laser interferometer scheme that has been demonstrated using conventional laboratory techniques.

In each of the two interferometers, the afocal telescopes compress samples of the starlight, which are directed toward the beamsplitter and spectrometers. See Fig. 2. To design a good beamsplitter for the intended wavelength range (0.25 to 0.9 μm) is difficult, especially if it must work at a large angle of incidence. Therefore, we have moved the spectrometer toward the target star to shift the incidence angle on the beamsplitter from 45 deg to 15 deg. As an added advantage, the angle of incidence at the fold flat M_6 changes in the same way. This reduces the polarization-dependent phase shift from this mirror, which is the only mirror on the star side of the beamsplitter that does not have a counterpart on the path from the other subaperture.

At the exit ports of the beamsplitter, the light is dispersed and focused onto a pair of detector arrays. See Fig. 3. When the star is on axis ($\delta = 0$), the signal at any given wavelength has equal intensity at the two beamsplitter exit ports. When the star is off axis ($\delta \neq 0$), constructive interference for a given wavelength at one port is complemented by destructive interference at the other port. At each port, an alternating pattern of constructive and destructive interference is observed. The resulting complementary channelled spectra form the basis for determining δ. Since the detectors in the array see narrow, contiguous portions of the optical spectrum, there are effectively a large number of narrow-band interferometers that collectively make use of all of the light. Because of their small bandwidths, these interferometers can function when the instrument is pointed several arcsec from the target. However, to keep the fringe visibility high, it is desirable to keep the pointing offset small compared to δ_N, the Nyquist angle, at which there are two detector pixels per fringe.

The channelled-spectrum approach has two distinct advantages over a system in which a single detector measures the white-light fringe. In the latter system, the absolute pointing error would have to be under 0.05 arcsec during observations (unless an active system of path compensation were included); white-light fringe detection would require an oscillating mirror to modulate the OPD (say at audio frequency). The fringe visibility would be substantially reduced at 1 arcsec, making the initial acquisition of the fringe more difficult. Thus, the use of the dispersed fringe simplifies the pointing system. The second advantage of the dispersed fringe approach is that there is additional information available in the channelled spectrum. This information can be used to separate targets that are closely spaced and might otherwise be confused, such as members of a binary system. An instrument utilizing this technique exclusively was proposed by Massa and Endal[11]. This additional information can be preserved to permit the reanalysis of the data after it has been determined that a target presumed to be simple had significant structure (*e.g.*, a binary). Further, the dispersed fringe approach makes optimal use of the photons near the intensity minima, where the derivative of signal with respect to stellar position is high and the shot noise is low.

The principal disadvantage of the dispersed fringe is that the large number of detector cells each contribute read noise. For bright targets, even those read rapidly to support the instrument fine pointing (Section 3.4), this is not a

problem. For faint objects, we integrate on the CCD chip up to five minutes. This results in a read noise comparable to the shot noise on sky background light, even when the spectrometer has a slit.

3.2. Internal measurements and systematic error

The diminution of systematic error is central to achieving the stated instrument performance and the mission science objectives. We address this problem at three levels: (1) stable materials and thermal control; (2) real-time metrology; and (3) the detection and correction of systematic error in conjunction with the global data analysis. The best materials fail by orders of magnitude to provide the long-term dimensional stability required to maintain each interferometer's optical path difference (OPD), in the absence of other means of control. Stable materials for the

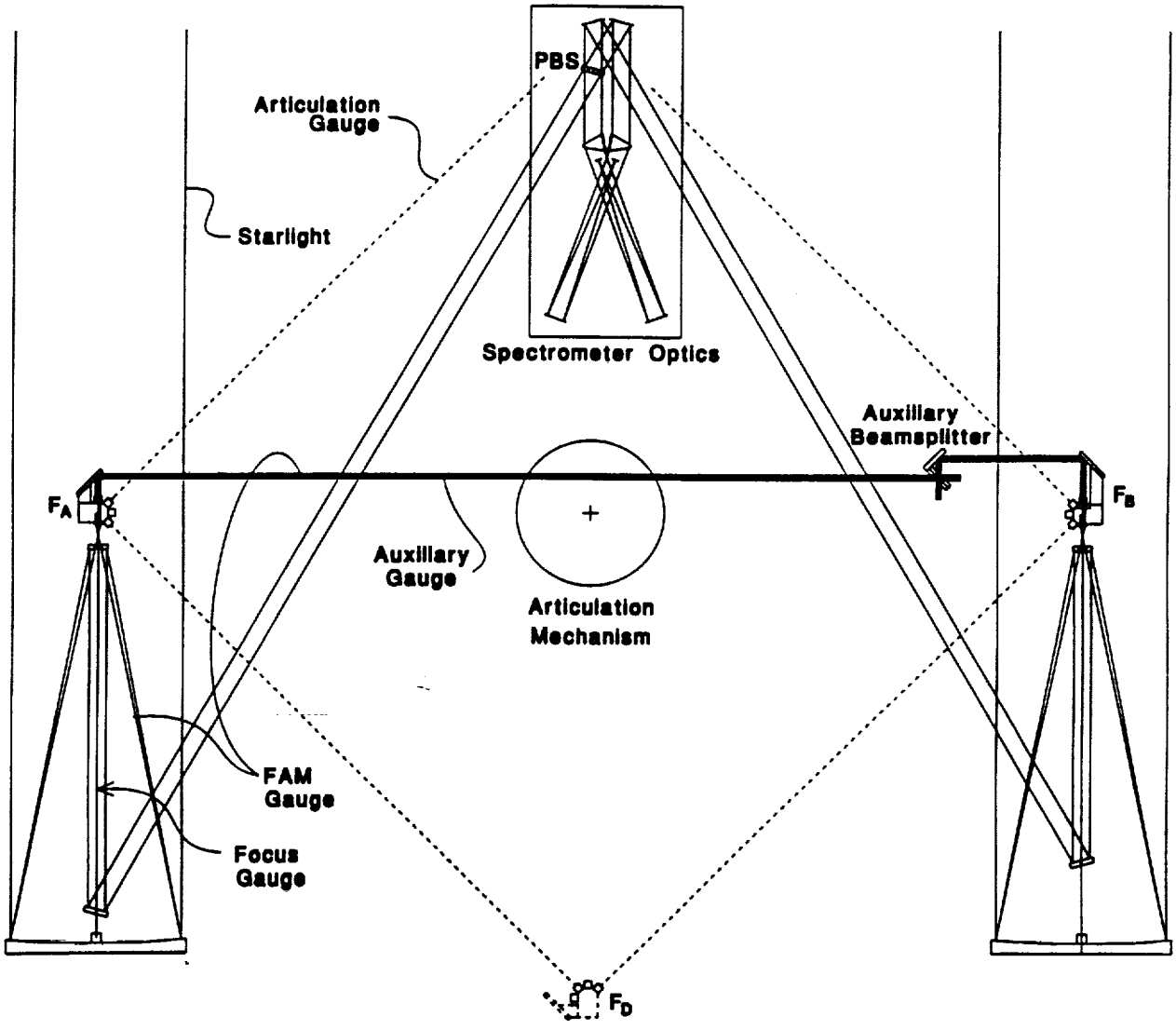

Figure 2. The optical paths in a single POINTS interferometer. Starlight beams enter at the top, are compressed by the left and right afocal telescopes, and combine at the primary beamsplitter PBS. Beams for FAM, the Auxiliary Servo, and the Focus Servo emerge from the Auxiliary Beamsplitter. The Auxiliary Servo beams are returned by cornercubes in fiducial blocks F_A and F_B, the Focus Servo beams are returned by cornercubes on the primary mirrors, and a portion of the FAM beams are diffracted at the primary to travel the same path as the starlight, combining at PBS, after which the FAM light is detected separately from the starlight. The other interferometer lies out of the plane of the drawing. Its fiducial blocks are F_C and F_D. F_D is shown, with dashed lines. Also shown dashed are four of the beams of the Baseline Articulation Angle Gauge. They measure distances from the fiducial points of F_A and F_B to those of F_C and F_D.

structural elements of the instrument serve to limit the dimensional changes that the metrology system must determine, and to control errors that are second order in component displacements. In a few places, we are forced to rely on material stability (over short times *i.e.*, up to a few hours). The instrument is designed so that such metering elements are small, and can be thermally isolated and regulated.

For a 2-m baseline, the nominal 5-μas uncertainty corresponds to a displacement of one end of the interferometer toward the source by 0.5Å = 50 pm (picometer = 10^{-12} m). Since similar displacements of internal optical elements are also important, the instrument requires real-time metrology of the entire starlight optical path at the few picometer level. We demonstrated one of the required laser gauges in the lab two years ago[12]. (Of course, we recognize that further development is required before the demonstration turns into a spaceworthy system.) The instrument relies on two kinds of laser-driven optical interferometers to determine changes in critical dimensions. The laser gauges can be grouped according to whether they measure distances internal to a starlight interferometer or distances between starlight interferometers.

The high-precision star position measurement is made with respect to the optical axis of the interferometer by determining from the channelled spectrum the difference in the optical paths from the target to the beamsplitter *via* the two sides of the interferometer. In turn, the position of this axis is determined (*i.e.*, defined) by the positions of the optical elements used to transfer the starlight. The metrology system must determine, to about 10 pm overall accuracy, the average change in the starlight OPD induced in each interferometer by all motions and distortions of all optical elements. Our approach is to use Full Aperture Metrology (FAM), which, in principle, provides three significant advantages over conventional approaches. (a) FAM is less complicated. (b) FAM measures more nearly the correct quantity. (c) FAM provides the basis for an operational definition of the direction of the interferometer baseline.

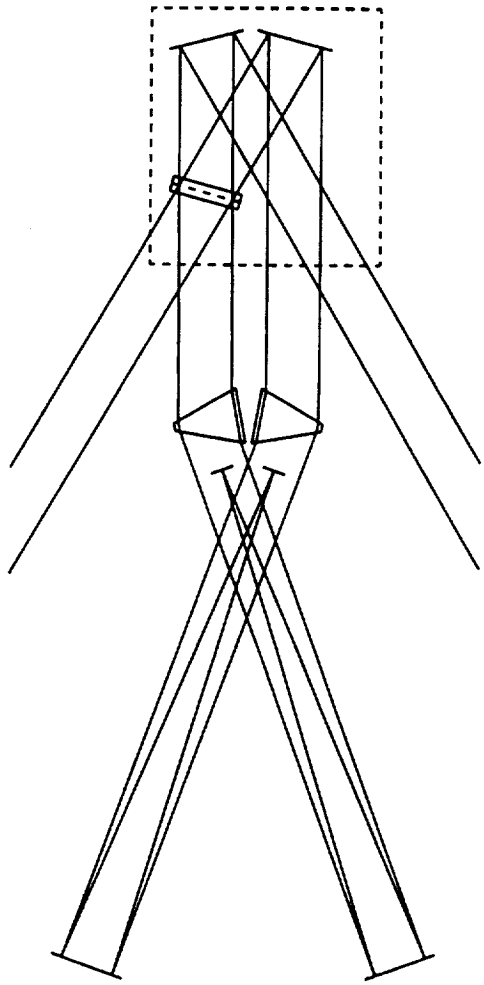

Figure 3. The POINTS beamsplitter and detector assembly. The detector arrays are above the prisms, and thus do not block the beams from the prisms to the off-axis parabolic mirrors. The components inside the dashed rectangle move together when the beamsplitter assembly is translated.

Figure 2 illustrates the preferred version of the technique, which requires two principal servos and one secondary servo. Modulated laser light is injected at the auxiliary beamsplitter, is deflected "down" by the top mirror in the fiducial block (Fig. 4), is focussed by the athermal lens in the fiducial block, and fully illuminates the primary mirror. A phase-contrast zone-plate hologram on the primary diffracts about 1% of the FAM light, so that it follows the starlight path, fully illuminating the optical elements that transfer the starlight. Thus, samples of FAM light from the two sides of the interferometer are brought together at the starlight beamsplitter. The resulting error signal drives the null-seeking FAM servo, which holds constant the OPD between the two beamsplitters *via* the two telescopes by moving the starlight beamsplitter assembly along the baseline direction. We anticipate the motion will be no more than a few microns. The associated transverse motion should be just a few nanometers and would have a completely negligible effect. Having the FAM light travel in the same direction as the starlight increases the scattered light on the starlight detectors but decreases the systematic error sensitivities.[13] This servo, in conjunction with the second servo (described below), surveys the starlight interferometer optics

into position with respect to the fiducial points, which are inside the fiducial blocks. These fiducial points are used to determine φ, the angle between the two interferometers' optical axes.

A second laser beam injected into the metrology beamsplitter parallel to the FAM beams similarly measures the difference in distances from that beamsplitter to each of two corner cube retroreflectors situated in the fiducial blocks. The resulting error signal drives the auxiliary servo, which regulates that path difference to a constant value by moving the auxiliary beamsplitter assembly in a direction parallel to the baseline. With both servos working, there is a small (under 1 mm) and constant difference between the distances from the starlight beamsplitter to the fiducial points, which are the apices of the retroreflectors inside the fiducial blocks. These servos can have small bandwidths because the time scale for distortion is long compared to a second, and because we require that vibrations of the OPD be small enough that they need not be tracked.

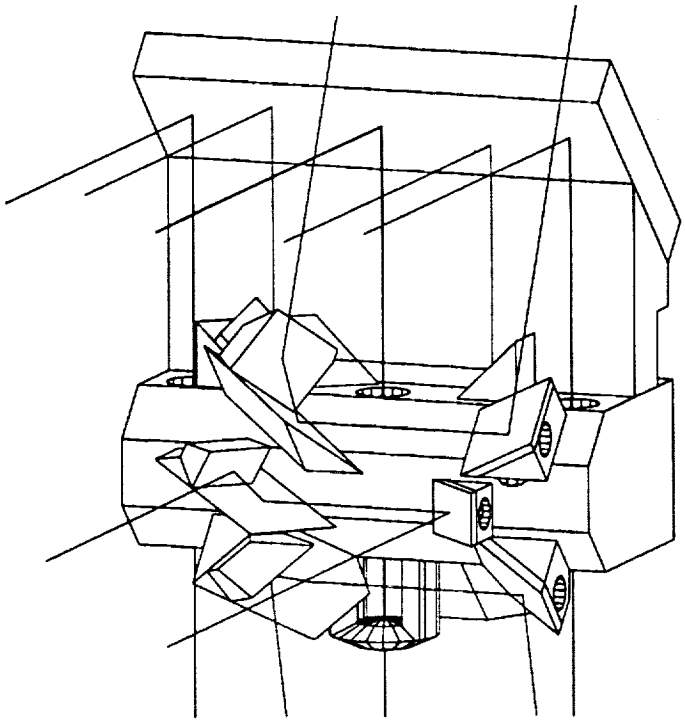

Figure 4. The fiducial block, including the central rays of the beams of metrology light that are affected by it. Five beams are seen reflecting from the 45 deg mirror at the top. These are for the focus gauge (outer pair), the auxiliary gauge (next pair), and FAM (central). The FAM beam is seen to emerge from the athermal lens at the bottom. Also visible are the four retrostrips. The top retrostrip returns the light to the auxiliary gauge. The other three work in conjunction with corresponding parts of the other three fiducial blocks to form the cavities that are used in the measurement of the distances between pairs of fiducial blocks.

We have shown that a change in the distance between the telescope primary and the athermal collimating lens linearly changes the FAM OPD by about 1% of the change of distance.[14] For this reason, we introduce a third servo related to FAM that moves the fiducial blocks equally and in opposite directions along the starlight optical path. (Note that, for such motions, the two overlapping illuminated regions on the auxiliary beamsplitter move in the same direction.) The sensor for this "focus servo" is a laser gauge that measures the difference of the distances from the auxiliary beamsplitter to the telescope primary mirrors *via* the fiducial block fold mirrors but excluding all other optics. With the auxiliary servo working, the focus servo measures the differential distance from the fiducial points to the primary mirrors. Note that the fiducial point is several cm from the athermal lens. This distance, which must be stable to about 0.1 nm, is metered by the body of the fiducial block, which is quite stable.

The fiducial blocks, the metrology and auxiliary beamsplitter assemblies, the athermal lens, and the optical bench structure pose the critical materials problems identified. To minimize changes of the size or shape of these, which would cause corresponding changes in the bias of the metrology system, they will be made of a stable material and kept in a thermally stable environment. For the fiducial blocks, we plan to use Premium ULE®; the beamsplitter material is fused silica. These items can make first-order contributions to an OPD error. For the optical bench, we plan to use graphite fiber in matrix. Optical bench misalignments appear only in second order in the OPD error[14].

Each fiducial block contains four incomplete hollow cornercube retroreflectors, constructed such that their apices coincide to within a few microns. The centroid of these apices is a fiducial point. The pair of fiducial points within each starlight interferometer define the pseudobaseline, which is held by the FAM servos at a small fixed angle (nominally

zero) to the real interferometer baselines. The angle φ between the pseudobaselines of the two interferometers (*i.e.*, the instrument articulation) is determined by the measurements of the six distances among four fiducial points in the system. The relation between this angle and the angle between the true baselines has been discussed.[15] (The small bias resulting from the angle between the pseudobaseline and the real baseline is determined routinely as part of the data analysis.)

3.3. Opto-mechanical considerations

Figure 5 shows the optical bench for one stellar interferometer. It has a box-like structure of graphite epoxy or graphite-cyanate composite. The latter is preferred for its milder outgassing characteristics. A cylindrical space near the center of the bench is for a large double preloaded tri-flex pivot that joins the two interferometers.[16] A similar flex pivot was made by the division of Perkin-Elmer, Inc., that is now Hughes Danbury Optical System, Inc., and flown on the Apollo Telescope Mount on Skylab, 1973-1974.[17,18] The two telescopes are mounted outboard, which offers

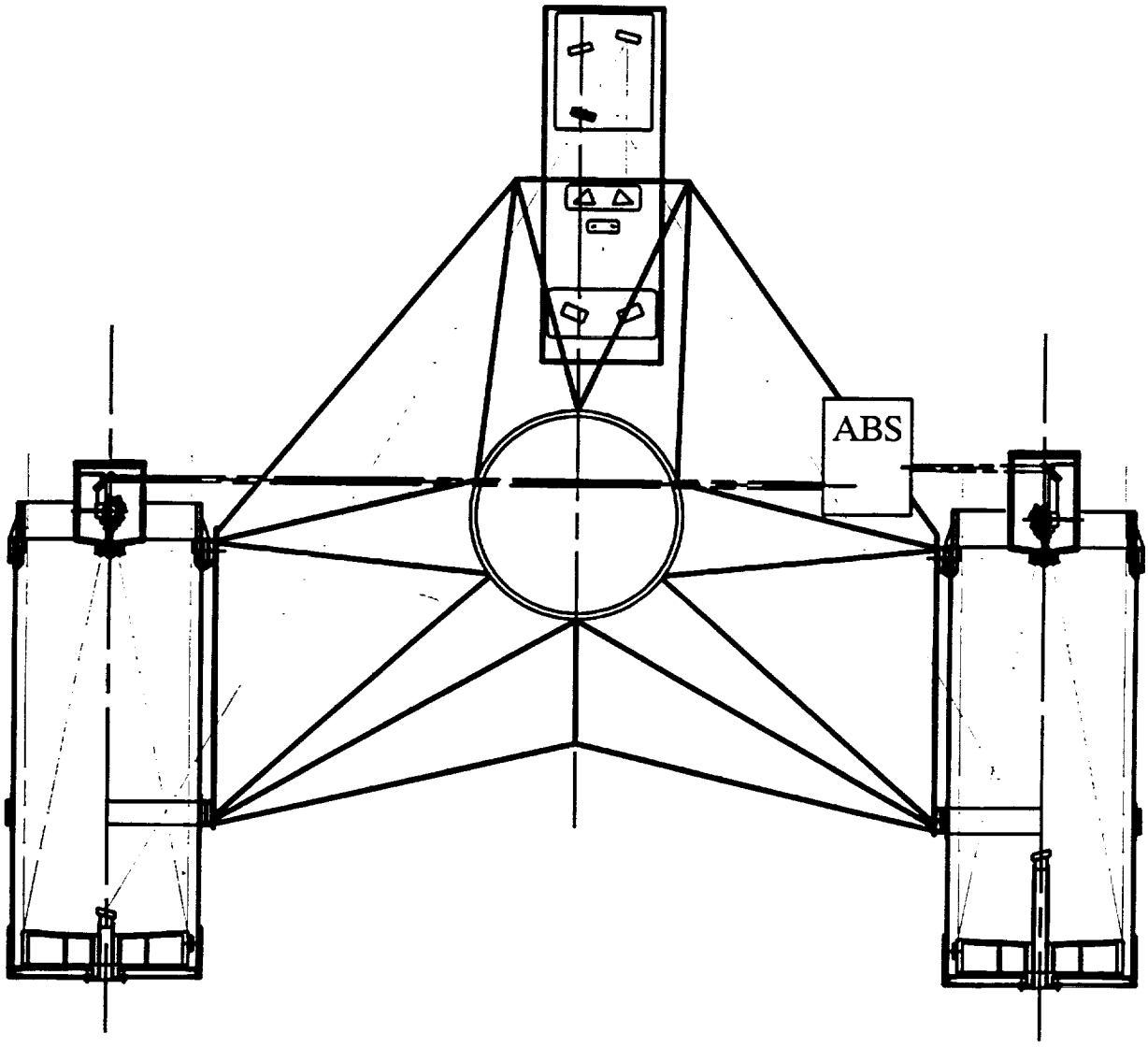

Figure 5. The optical bench. (F. Bovenzi, Itek) The large circular opening near the center of the bench is for the flex-pivot that joins the benches.

advantages in comparison to a design that engulfs the telescopes within the optical bench. As separate units, the telescopes can be aligned internally before being joined to the optical bench. Each telescope is joined to the optical bench at three points. These joints provide for a relatively simple alignment of the telescope assembly to the bench. In addition to lowering integration and testing costs, the design shown in Fig. 5 is believed to save mass, although a comparison of developed exemplars of the two approaches has not been performed.

Within each telescope is a lightweighted primary mirror mounted to the telescope tube by three flexures as shown in Fig. 6. Each flexure constrains two degrees of freedom but is soft in the other four degrees; the set of three locates the mirror without transferring stress to the mirror. This approach was used for the Teal Ruby telescope.[19] At the other end of the telescope tube, the fiducial block and secondary supports are held in place by three-leg spiders as shown in Fig. 7. The fiducial block is suspended within the double-wall shield can by six stingers (flexure devices that transmit negligible torque, and transmit force only along their length) in groups of one, two, and three. A detail of the connection between the fiducial block and the stingers is shown in Fig. 3b of Schumaker *et al.*, which shows an Invar button bonded to a glass pedestal.[20] The latter, which is bonded to the fiducial block, is intended to filter stresses induced by the Invar button and stingers and impart to the fiducial block only the net force and torque from the stingers. This should be principally forces along the directions of the attached stingers.

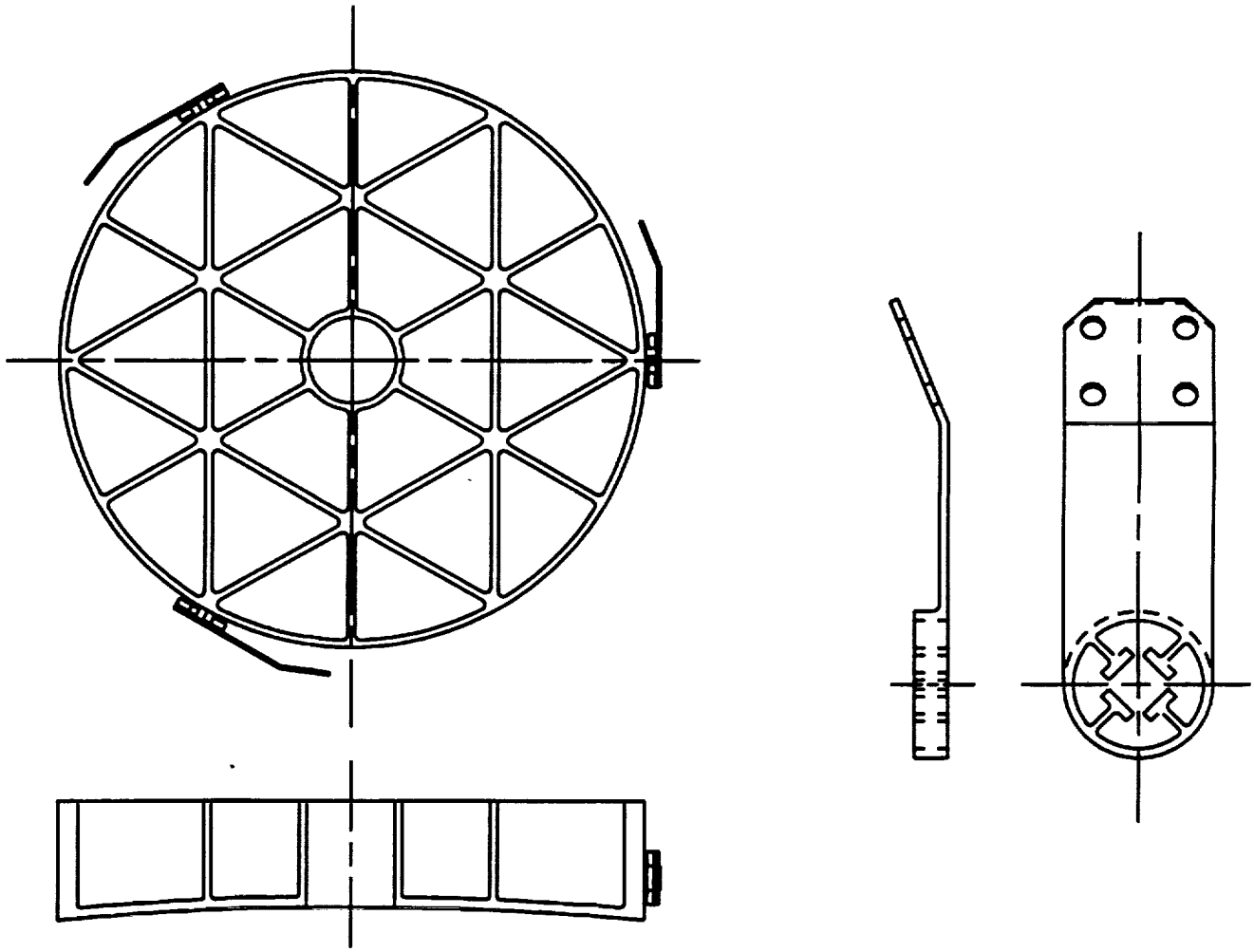

Figure 6. The primary mirror and support. (Itek) Left: the primary mirror, showing a pattern of material removal for mass reduction, and the flexural supports. Right: one of the flexures for supporting the mirror.

3.4. Detectors, spectrometer, and instrument pointing

There are four principal questions concerning detectors, the spectrometer, and pointing: (1) How far from the target direction can the instrument point and still detect the target? (2) What is the integration time? (3) What is the effect on the information rate of a pointing offset? (4) What is the limiting magnitude of the instrument? As $|\delta|$ is increased from zero, the number of fringes on the detector array increases, and the fringe visibility V decreases because each pixel averages over an increasingly large portion of a fringe. The information content of the data is monotonic with V, both of which are zero at $\delta=2\delta_N$, where there is one fringe per pixel. For the current design, δ_N=9.1 arcsec. The information content falls rapidly with decreasing V near V = 1, so the visibility must be kept high.

Equation 1 is a simplified model of the factors that determine the integration time for an observation:

$$\frac{\sigma(\delta)}{5\ \mu\text{as}} = \frac{10^{(m_b-10)/5}}{\left(\frac{T}{5777\ \text{K}}\ \frac{\alpha_1}{0.80}\ \frac{\alpha_2}{0.78}\ \frac{\eta}{0.15}\ \frac{\tau}{33\ \text{s}}\right)^{1/2}\ \frac{D}{35\ \text{cm}}\ \frac{L}{2\ \text{m}}} \qquad (1)$$

where m_b is the target star's bolometric magnitude, τ is the integration time, α_1 is a bandwidth factor that depends on T, the temperature of the target star, α_2 is a visibility factor, η is the overall instrument photon detection probability, D is the diameter at a single subaperture, and L is the baseline length. If all wavelengths of radiation were used, we would have α_1=1; and for V=1, α_2=1. For POINTS, with T=5777 K and a bandwidth range of 0.9 to 0.25 microns, we find α_1=0.80; and we estimate α_2=0.78. In the actual model, we perform a numerical quadrature over the optical bandpass to determine the information rate and use this to find the integration time. The factors α_1 and α_2 are found by leaving out the associated components of the integrand. For the CCD, we used a read noise of 3 electrons rms and a probability of 50% (independent of wavelength) for detecting a photon that hits the array.

We have found that the fringes can be held sufficiently stable that we can use an integrating detector such as a CCD. CCDs offer high quantum efficiency; there is a wide base of experience of their use in space, and rapid continuing development. The instrument pointing must display sufficient accuracy and stability that the visibility of the fringe is not significantly degraded. Our present plan calls for the instrument to include a fine-pointing and isolation system, and for the "bright-star interferometer" (which must be designated for each measurement) to provide angle error information to the fine-pointing system. That interferometer will need a target star as bright as $m_{BS} \approx 10$ and rapid readout of its detector array. To have the unit-gain bandwidth of the fine-pointing servo at 5 Hz would require a sampling rate of about 50 Hz. At this rate, each sample of a mag 10 star would have a statistical uncertainty of ≈ 400 μas. The detector in the "faint-star interferometer" need not be read rapidly, but only often enough that (a) it does not saturate and (b) cosmic-ray hits do not invalidate too many pixels of a single frame.

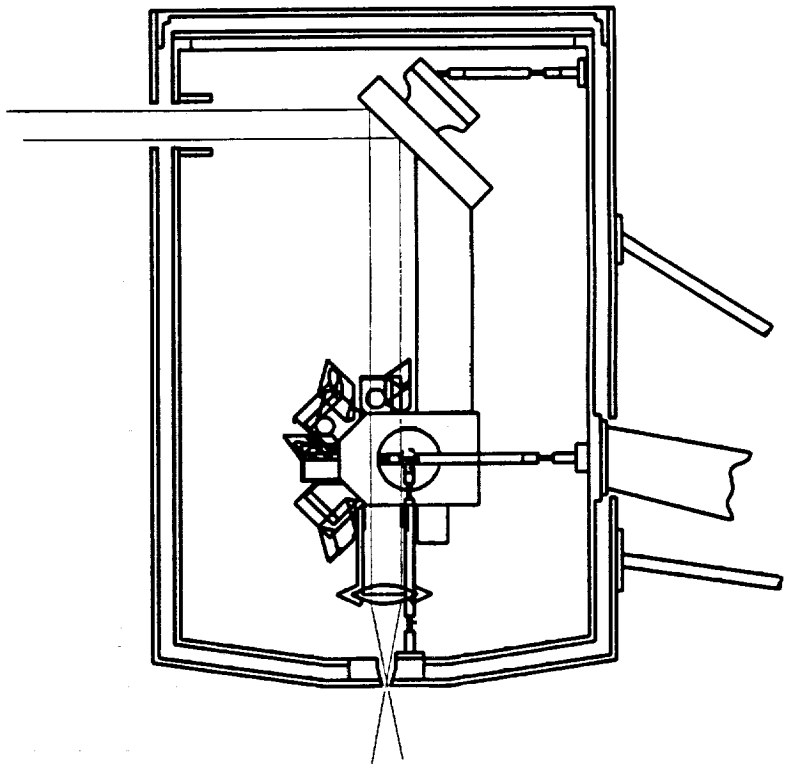

Figure 7. The fiducial block and enclosure. (Itek) In this Picasso-esque drawing, a set of spider arms has been rotated 90 deg into the instrument plane to show the design.

A prime candidate for the fine-pointing and isolation actuator is a "hexapod," such as the VAMP, which is under development at Harris Corporation.[21] Its six struts each contain a length actuator and a pair of accelerometers. The accelerometers at the "noisy end" operate in feed forward, while those at the "quiet end" operate in feedback to the central actuator. Additional information from the instrument star tracker and the bright-star interferometer would be blended with the accelerometer-based feedback information.

During initial target acquisition, star trackers in the instrument will locate the target and provide angle and angle-rate information for the fine-pointing system. This information would be used to reduce the offset and rotation rate to below the threshold for detecting starlight fringes. Similar information from the star trackers on the spacecraft bus will be used by the ACS. Biases in the ACS will be determined as part of the ground-based analysis of spacecraft engineering data and used to correct the spacecraft software algorithms as needed.

The present slitless spectrometer design is intended for bright, isolated targets. Dispersion is provided by a fused silica prism, with an apex angle of 35 deg, operated at minimum deviation. An antireflection coating limits the reflective loss at each prism surface to about 1.5%. Over the optical passband of 0.25 to 0.9 microns, the deviation changes by 2.1 deg and the dispersion ($d\theta/dv$) varies by a factor of three. A single off-axis parabolic mirror of 27 cm focal length images the channelled spectrum onto a detector array 512 pixels long. Each pixel is 20 μm square, and subtends 1.5 arcsec on the sky. (These pixels are somewhat larger than the Airy spot, but spectrometer resolution still contributes only minutely to integration time.) There may be a need for up to 100 pixels in the cross-dispersion direction to observe multiple targets in crowded fields. In addition, there may be a shaded readout area equal in size to the exposed area. It may be beneficial to use a 512 × 512 pixel CCD, ignoring the extra pixels, if it permits the use of an off-the-shelf device.

We plan to operate the instrument with about five fringes on the detector array to avoid the loss of visibility (and thus of information) that comes from a large number of fringes and the difficulties with systematic error that come from too few fringes. With 5, 20, and 100 fringes on the detector, the integration time is 32.6, 33.9, and 59.6 sec, respectively, for a magnitude 10 star. On the bright star, the limiting magnitude is set by read noise at the 50 Hz rate, and is 10. On the faint star, the limiting magnitude is set by sky background, and is 14. If we add a slit to the spectrometer, the faint star limiting magnitude becomes 17.

4. SPACECRAFT AND MISSION

The deployed spacecraft is shown in Fig. 1. The two pairs of ports used by the stellar interferometers are visible. The round ports are used by the interferometer that is fixed to the bus (except for the motions of the fine-pointing and isolation system). The elongated ports are used by the interferometer that moves with respect to the bus as a result of the inter-interferometer articulation. Behind the ports, but not shown, are baffles to limit the loss of heat and, more importantly, to limit the change of heat loss associated with the exposure of the ports to the solar shield.

Visible on the bus are the four Hubble-type reaction wheels. These are selected for their high torque and angular momentum storage capacity, of value for the rapid slews needed for an efficient ASEPS-1 mission, and for their established low vibrational noise. The ACS also includes a set of cold N_2 thrusters, intended for unloading the reaction wheels. However, most unloading will be by intentionally produced solar-radiation torque. Also visible are the two sets of antennas for the spacecraft tracking beacon and moderate-rate communication with the ground. The deployed shield provides a dark and thermally benign environment for the instrument and supports the array of GaAs solar cells.

The solar shield is connected to the bus by a boom that has two parts, a long straight section that unfolds during deployment and a curved section. The bending and twisting of the boom-shield have natural frequencies of at least 2 Hz. At both ends of the curved section, there are gimbal actuators. The boom has a square cross-section 18 cm on a side and 0.3 cm thick. Both of the gimbal axes pass through a point near the spacecraft (bus plus instrument) center of mass. The gimbal actuators permit the spacecraft to rotate while keeping the solar shield pointed toward the Sun. In conjunction with the reaction wheels, the gimbals allow the shield to point toward the Sun or to be displaced to produce radiation pressure torque for unloading the reaction wheels (two axes only). These actuators must be capable of 0.1 deg accuracy over a 345 deg (or larger) range of motion, and have a lifetime consistent with spacecraft slews totalling about 0.6 million radians (about 350 slews per day for 10 years, each slew averaging about 25 deg). The baseline design is a standard stepper motor driving a (200:1) harmonic-drive reducer. (See Agronin,[16] Fig. 14.) Each gimbal axis has bearings separate from the actuator to support the main loads, the actuator driving the axis through a flexible coupling.

Similar actuators have been used to drive solar panels on the Magellan and TOPEX spacecraft.

Table 2. Spacecraft Mass

Component	Mass (kg)
Instrument	240
Instrument housing	130
Bus	680
Solar shield and boom	170
Launch equipment	130
Subtotal	1350
Contingency (30%)	405
Total	1755

The nominal power requirement for the spacecraft, including power to operate the power conditioning system, is 675 Watts average (766 peak). To that we add a 30% contingency margin and 220 Watts capacity to recharge the battery after solar occultation: 1098 average (1216 peak) Watts. For the POINTS mission, we have selected GaAs/Ge solar cells, which yield 105 W/m^2 at the end of 10 years in service in the 100,000 km orbit baselined for POINTS. With the available 18 m^2 of shield, the spacecraft could develop 1900 Watts. Alternatively, we could populate 64% of the available area and just meet the peak load requirement at the end of the mission. Even the latter is a conservative design. Consider the situation at the end of the mission, and assume that we did not need the 30% contingency. Then the design peak would be 986 Watts and it would suffice to cover 52% of the shield with cells. However, if it were necessary, we could recharge the battery during off-peak times and at a lower rate than 220 Watts. Thus we could function with a peak capacity of only 766 Watts. (Solar occultations are limited to two seasons. There are likely to be two or three occultations per season and they would last under two hours. Recharge could be completed in under a day.) Thus, at the end of the mission we would have nearly 30% "excess" capacity.

The nominal orbit under consideration for POINTS is circular with a radius of 100,000 km, corresponding to a period of about 3.6 days. The baseline launch vehicle for POINTS is an Atlas IIAS with a Centaur upper stage and a Star 37FM (Thiokol) solid-rocket motor for orbit circularization. This combination is capable of delivering a payload of approximately 1740 kg to a circular orbit of 100,000 km radius at the minimum-energy inclination of 28.5 deg with respect to the equator. (This assumes a launch from Florida.) In deriving this payload limit, we include a deduction of 7.5% of the Atlas-Centaur capability for Launch Vehicle Contingency Reserve, Launch Vehicle Mission-Peculiar Reserve, and Launch Vehicle Project Manager's Reserve. In addition, the 99%-confidence Flight Performance Reserve is included (*i.e.*, the flight performance is assumed to be well below average, at a value that should be exceeded with a probability of 99%). The current best estimate for the POINTS payload is about 1350 kg without contingency, or 1755 kg with a 30% contingency included, a good match to the capabilities of the chosen launch vehicle. See Table 2. Changing the inclination by 20 deg would reduce the payload capability by about 100 kg. (The orbital inclination may also be changed during the circularization burn of the Star 37FM.)

Figure 8 shows POINTS folded into the launch configuration. The launch will be into a transfer orbit with an altitude of about 167 km, after which the Centaur upper stage will be fired to insert POINTS into an elliptical transfer orbit with an apogee of approximately 100,000 km. Following separation from the Centaur, the solar shield will be deployed partially (Fig. 9) in order to provide a required power of approximately 340 Watts during the 17-hr cruise to the 100,000-km radius; the spacecraft will be 3-axis-stabilized during this long cruise. Just prior to ignition of the Star 37FM for orbit circularization, a small spin-up motor will be fired to provide a spin rate of a few RPM for the 60-second circularization burn, and a similar motor will be fired following the circularization to de-spin the spacecraft, which then will be returned to its 3-axis stabilized mode. Following the circularization, the propulsion module will be jettisoned, and deployment of the solar shield will be completed. Given the magnitudes of the expected errors in both the orbit-injection and circularization burns, the perigee and apogee should be within 5% of the nominal values, well within the acceptable range for the POINTS mission.

The right angle orientation of the two POINTS interferometers accentuates the need to model astrometric measurements for the effect of stellar aberration, which produces an angular offset that scales linearly with the spacecraft velocity and the sine of the angle between the target stars. In order for the error in the model of this offset to be smaller than 1.0 μas, the POINTS spacecraft velocity must be determined to better than 1.5 mm/s. In fact, the strategy described below appears to be capable of determining the spacecraft velocity to better than 0.3 mm/s (0.2 μas contribution to the astrometric error). In high Earth orbit, the primary external source of disturbance to the spacecraft acceleration is solar

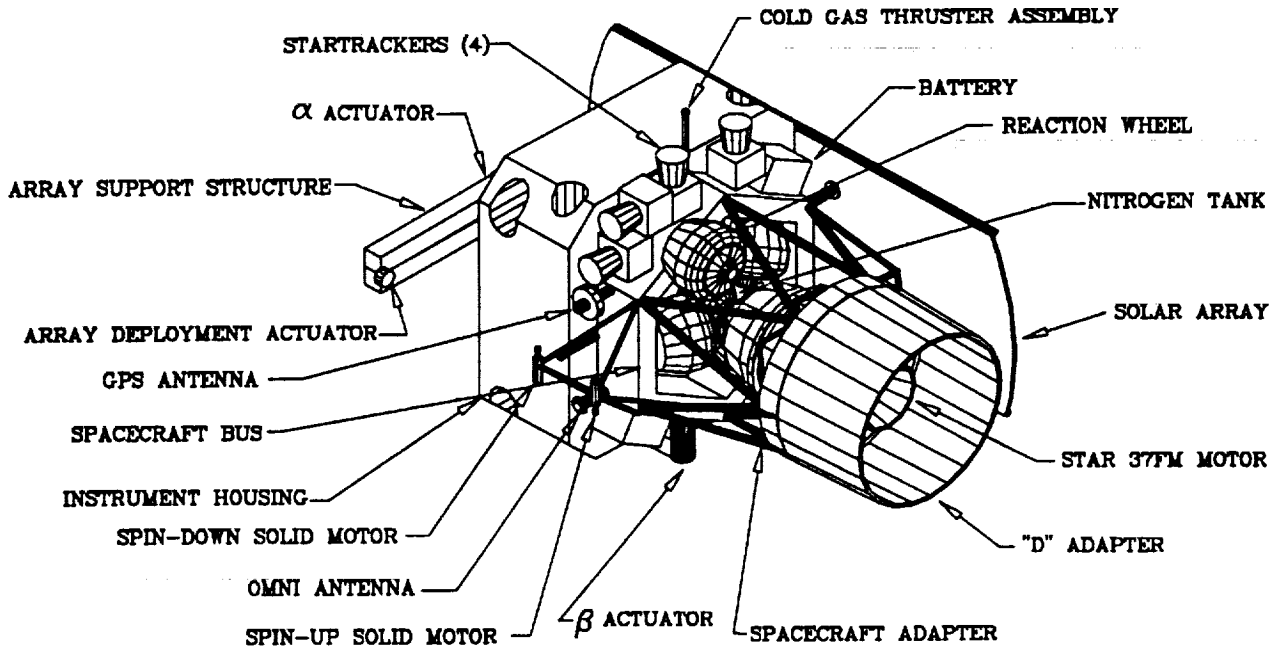

Figure 8. The spacecraft in launch configuration. (D. Noon, JPL)

radiation pressure, the effects of which can be modeled quite accurately for POINTS because of the simple geometry of its Sun-facing side. Effects from atmospheric drag and anomalies in Earth's gravitational field, which dominate the unmodelled spacecraft acceleration in low orbits, are negligible. The typical rate of leakage from the cold-gas system and solar wind pressure also will yield accelerations that are small compared to the uncertainties in the acceleration due to solar radiation pressure.

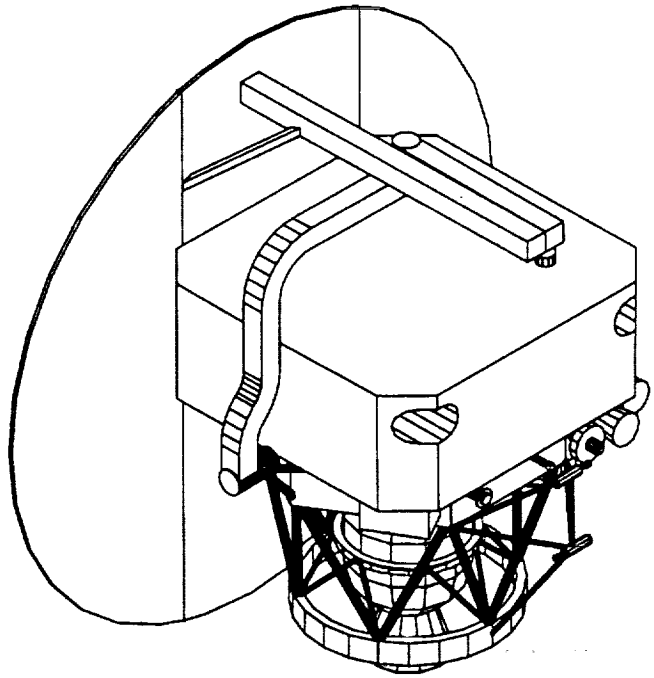

Figure 9. The spacecraft in cruise configuration. (D. Noon, JPL) The solar array, but not its support boom, is deployed, permitting the spacecraft to generate electrical power.

At a radius of 100,000 km, POINTS would be well outside the constellation of Global Positioning System (GPS) satellites, which have orbital radii of about 27,000 km. Although this makes it impractical to determine velocity by using an on-board GPS receiver, an alternative technique can be used in which POINTS carries a beacon and mimics a GPS satellite[22]. This alternative is predicted to meet the velocity requirements rather easily[23]. POINTS would carry a GPS-like beacon having multiple tones in the frequency ranges of 1.2-1.6 GHz (L band) or near 16 GHz (Ku band); the multiple tones are used to correct for ionospheric effects. The beacon would be tracked by 8-channel GPS receivers located around the world, with each receiver simultaneously tracking seven GPS satellites and POINTS. Figure 10 displays the basic velocity-determination results predicted by a covariance analysis. Using only the six TOPEX tracking sites and tracking for only two hours out of every eight, the predicted velocity error for POINTS would be about 0.1 mm/s after a single 4-day orbit. Even after

another six days with no tracking data, the velocity uncertainty would grow to only 0.25 mm/s, still easily meeting the requirement. Thus, a total of 24 hours of tracking, poorly distributed over 16 days is more than sufficient; it is likely that the POINTS velocity requirements could be met with a tracking duty cycle well under 10%.

The spacecraft and ground hardware required for the orbit determination would be simple and have been analyzed by Dunn and Young[24]. The spacecraft would broadcast a signal of about 1.5 Watts through one of a pair of switched nearly omni-directional antennas. Since nearly omni-directional antennas could be used, there would be no need to interrupt the scientific observing to point these antennas at the Earth. Occasional interruptions in the beacon signal would be required in order to change from one antenna to the other, but this is of little consequence given the low requirement for the overall tracking duty cycle. Simple modeling of the antenna position (and phase center) relative to the spacecraft center of mass should suffice to reduce all beacon data to the proper reference frame. In order to enable the necessary coherent integration time of about one second, an ultra-stable oscillator with frequency stability $\delta f/f \approx 7\times10^{-11}$ over one second would be needed on board for the 1.6 GHz option, while a frequency stability of 7×10^{-12} would be required for the 16-GHz frequency. A stability of 10^{-12} may enhance Doppler tracking or reduce operations cost; this level of stability is available on GPS spacecraft from rubidium standards, which come in palm-sized packages. However, we have not studied the use of Doppler data.

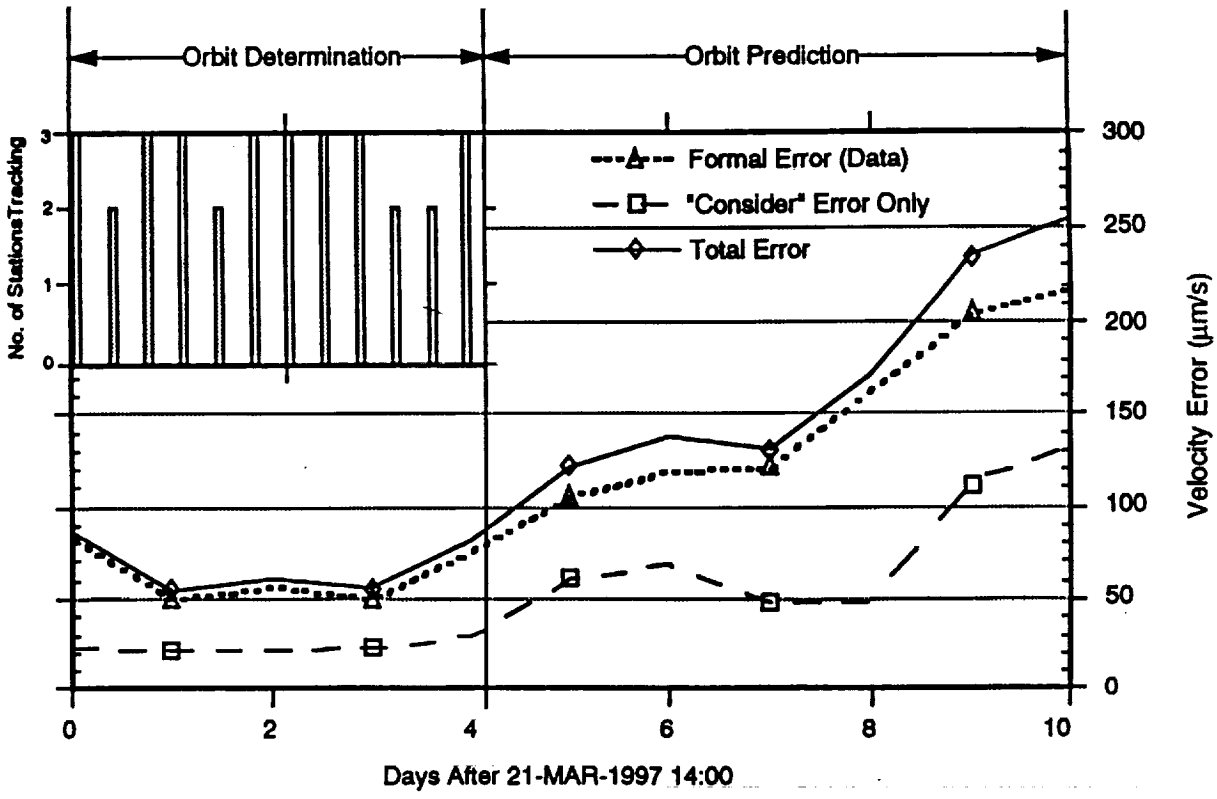

Figure 10. Results of an orbit-determination study. (C. Dunn and L. Young, JPL) The curve of velocity uncertainty is approximately symmetric around the center of the four-day period during which the tracking data are collected.

5. ACKNOWLEDGEMENTS

At SAO, the work was supported by the NASA Solar System Exploration Division through the Planetary Instrumentation Definition and Development Program Grant # NAGW 2497 and by the Smithsonian Institution. At JPL, the work was supported by the NASA Solar System Exploration Division. We thank our colleagues at Itek Optical Systems, Inc., for their numerous contributions to the POINTS design. The authors gratefully acknowledge the careful preparation of the camera-ready text by S.A. Silas.

6. REFERENCES

1. M.A.C. Perryman, E. Høg, J. Kovalevsky, L. Lindegren, C. Turon, P.L. Bernacca, M. Crézé, F. Donati, M. Grenon, M. Grewing, F. van Leeuwen, H. van der Marel, C.A. Murray, R.S. Le Poole, and H. Schrijver, "In-orbit performance of the Hipparcos astrometry satellite," Astron. Astrophys., 258, pp. 1-6, 1992.

2. E. Høg, "Astrometry and Photometry of 400 Million Stars Brighter than 18 Mag," Developments in Astrometry and Their Impact on Astrophysics and Geodynamics, I.I. Mueller and B. Kolaczek, eds., IAU, pp. 37-45, 1993.

3. L. Lindegren, M.A.C. Perryman, U. Bastian, J.C. Dainty, E. Høg, F. van Leeuwen, J. Kovalevsky, A. Labyrie, S. Loiseau, F. Mignard, J.E. Noordam, R.S. Le Poole, P. Thejil, and F. Vakill, "GAIA - Global Astrometric Interferometer for Astrophysics," in these proceedings.

4. R. Epstein, and I.I. Shapiro, "Post-post-Newtonian Deflection of Light by the Sun," Phys. Rev. D., 22, pp. 2947-2949, 1980.

5. E. Fishbach, and B.S. Freeman, "Second-order contribution to the gravitational deflection of light," Phys. Rev. D., 22, p 2950, 1980.

6. G.W. Richter, and R.A. Matzner, "Gravitational deflection of light at 1 1/2 PPN order," Astrophys. and Space Sci., 79, 119, 1981.

7. TOPS: Toward Other Planetary Systems, A Report by the Solar System Exploration Division, Bernard Burke, ed., NASA, Washington, DC, November 1992. [See page 18.]

8. The Decade of Discovery in Astronomy and Astrophysics, National Research Council, National Academy Press, Washington, DC, 1991.

9. R.D. Reasenberg, R.W. Babcock, J.F. Chandler, M.V. Gorenstein, J.P. Huchra, M.R. Pearlman, I.I. Shapiro, R.S. Taylor, P. Bender, A. Buffington, B. Carney, J.A. Hughes, K.J. Johnston, B.F. Jones, and L.E. Matson, "Microarcsecond Optical Astrometry: An Instrument and Its Astrophysical Applications," Astron. J., 32, pp. 1731-1745, 1988.

10. "Astrometric Interferometry Mission Strawman Science Program," Space Interferometry Science Working Group [established by the Astrophysical Division of NASA and chaired by S. Ridgway], 5 July 1992.

11. D. Massa and A.S. Endal, "An Instrument for Optimizing a Spaceborne Interferometer: Application to Calibrating the Cepheid Distance Scale," Astron. J., 93(3), p. 760, 1987.

12. R.D. Reasenberg, R.W. Babcock, M.C. Noecker, and J.D. Phillips, "POINTS: The Precision Optical INTerferometer in Space," The Proceedings of the ESA Colloquium on Targets for Space-Based Interferometry, European Space Agency, Beaulieu-sur-Mer, France, 13-16 October 1992, ESA Publications Division, Noordwijk, The Netherlands, ESA-SP-345, pp. 59-69, December 1992.

13. M.C. Noecker, J.D. Phillips, R.W. Babcock, R.D. Reasenberg, "Internal laser metrology for POINTS," The Proceedings of the SPIE Conference # 1947 on Spaceborne Interferometry, (Orlando, FL, April 14-16, 1993), Vol. 1947, pp. 174-187, 1993.

14. M.C. Noecker, M.A. Murison, R.D. Reasenberg, "Optic-misalignment tolerances for the POINTS interferometers," The Proceedings of the SPIE Conference # 1947 on Spaceborne Interferometry, (Orlando, FL, April 14-16, 1993), Vol. 1947, pp. 218-231, 1993.

15. R.D. Reasenberg, R.W. Babcock, M.C. Noecker, and J.D. Phillips, "POINTS: The First Small Step," The Proceedings of the SPIE Conference # 1947 on Spaceborne Interferometry, (Orlando, FL, April 14-16, 1993), Vol. 1947, pp. 12-29, 1993. [See Appendix for discussion of relationship between the baseline and the pseudobaseline.]

16. M.L. Agronin, "Precision actuators for spaceborne interferometers: a tutorial," The Proceedings of the SPIE Conference # 1947 on Spaceborne Interferometry, (Orlando, FL, April 14-16, 1993), Vol. 1947, pp. 140-160, 1993.

17. A. Wissinger, private communication, Hughes Danbury Optical Systems, Inc., (203-797-6259), 1993.

18. J.A. Eddy, A New Sun: The Solar Results from Skylab, NASA SP-402, NASA, Washington, DC, p. 47, 1979.

19. J.W. Pepi, R.J. Wollensak, "Ultra-lightweight fuse silica mirrors for a cryogenic space optical system," The Proceedings of the SPIE Conference # 183 on Space Optics, Vol. 183, pp. 131-137, 1979.

— J.W. Pepi, M.A. Kahan, W.H. Barnes, R.J. Zielinski, "Teal Ruby — design, manufacture and test," The Proceedings of the SPIE Conference # 216 on Optics in Adverse Environments, Vol 216, pp. 160-173, 1980.

20. B.L. Schumaker, M. Agronin, G-S. Chen, W. Ledeboer, J. Melody, D. Noon, and J. Ulvestad, "Spacecraft and mission for the Precision Optical INTerferometer in Space (POINTS)," The Proceedings of the SPIE Conference # 1947 on Spaceborne Interferometry, (Orlando, FL, April 14-16, 1993), Vol. 1947, pp. 58-72, 1993.

21. D. Hyland, private communication. Harris Corporation, Government Aerospace Division, Melbourne, Florida, (407-729-2138), 1994.

22. S.L. Lichten, C.D. Edwards, L.E. Young, S. Nandi, C. Dunn, and B.J. Haines, 1993, "A demonstration of TDRS orbit determination using differential tracking observables from GPS ground receivers," AAS Paper 93-160, AAS/AIAA Spaceflight Mechanics Meeting, Pasadena, CA, February 1993.

23. B. Haines, and S. Lichten, "POINTS orbit determination with GPS-like beacon," JPL IOM 335.8-92-036, 1992.

24. C. Dunn and L.E. Young, "POINTS Navigation Beacon Strawman Design," JPL IOM 335.9.003-93, 1993.

Newcomb, a scientific interferometry mission at low cost

Robert D. Reasenberg, Robert W. Babcock, and James D. Phillips

Smithsonian Astrophysical Observatory
Harvard-Smithsonian Center for Astrophysics
60 Garden Street, Cambridge, MA 02138

Kenneth J. Johnston

United States Naval Observatory
34th Street & Massachusetts Avenue, N.W., Washington, DC 20392

Richard S. Simon

National Radio Astronomy Observatory
520 Edgemont Road, Charlottesville, VA 22903-2475

ABSTRACT

Newcomb is a design concept for an astrometric optical interferometer with nominal single-measurement accuracy of 100 microseconds of arc (μas). In a 30 month mission life, it will make scientifically interesting measurements of O-star, RR Lyrae, and Cepheid distances, probe the dark matter in our Galaxy *via* parallax measurements of K giants in the disk, establish a reference grid with internal consistency better than 50 μas, and lay groundwork for the larger optical interferometers that are expected to produce a profusion of scientific results during the next century. With an extended mission life, Newcomb could do a useful search for other planetary systems.

The instrument is a highly simplified variant of POINTS. It has three (or four) interferometers stacked one above the other. All three (four) optical axes lie on a great circle, which is also the nominal direction of astrometric sensitivity. The second and third axes are separated from the first by fixed "observation angles" of 40.91 and 60.51 deg. The fourth axis would be at either 70.77 or 78.60 deg from the first. Each interferometer detects a dispersed fringe (channelled spectrum), which falls on a short CCD detector array. The optical passband is from 0.9 to 0.3 microns. We will move the beamsplitter assembly along the baseline direction up to ±2 mm to compensate the change in the optical path difference associated with a target away-from the nominal interferometer axis. This is a recent design change that adds complexity (moving parts in the interferometer) to achieve adequate field of view; it also enhances astrometric accuracy. With a nominal baseline length of 30 cm, the deviation limit is reached by a star ±23 arc min from the optical axis. The instrument will be constructed of stable materials such as ULE glass, and have minimal internal moving parts and simple laser metrology.

A reference frame can be constructed using stars located in a regular pattern on the sky. We start with the 60 points that are vertices of the regular truncated icosahedron. The instrument axis separations are chosen as separation angles of the figure such that for each vertex there are four other vertices at the chosen angle. (There is no angle offering higher multiplicity.) To the original set of 60 points, we add two additional such sets by rotating the figure ±20.82 deg. With such a grid of 180 stars, we have shown POINTS-like grid lock-up even with large Sun-exclusion angles (of up to 75 deg). In the covariance studies, we assumed nine quarterly observation series and five bias parameters per series per observation angle; we estimated position, proper motion, and parallax for each star. In an extension of the study, we eliminated stars at random from the set and found that there was stable behavior with as few as half the stars in the grid. Further, with 120 stars in the grid, the statistical uncertainty of star position increased by only 31% due to degeneracy (*i.e.*, with constant number of observations.)

As with POINTS, additional stars can be observed with respect to the grid. With three interferometers and a full grid and without exceeding the deviation limit, the region accessible for observing with respect to at least two grid stars is over 85% of the sky outside of the Sun exclusion zone. This observable region can be enlarged by either including more sets of 60 points in the reference star grid, or adding the fourth interferometer, or increasing the allowed deviation.

2. INTRODUCTION AND INSTRUMENT ARCHITECTURE

Newcomb is a design concept for an astrometric optical interferometer with nominal single-measurement accuracy of 100 microseconds of arc (μas). It is a low-cost derivative of POINTS (Reasenberg, *et al.* in these proceedings) intended for early demonstration of some interferometer technology and a reduced (from the POINTS goals) but significant scientific program in addition to the principal goal of establishing a high precision reference grid. The instrument will measure the angular separation of a pair of mag 9 stars to 100 μas in about five minutes. In December 1992, a collaboration was established between Smithsonian Astrophysical Observatory and Naval Research Laboratory to develop Newcomb for the Navy's Space Test Program (STP)[1]. The United States Naval Observatory joined the collaboration in 1993. The intent was that the instrument would be kept simple and the mission, of short duration for an astrometric investigation, nominally 30 months.

The instrument comprises three or four Michelson stellar interferometers, each with a dispersed-fringe detection system. Each interferometer baseline will be parallel to the instrument's "principal plane." As we picture the construction, there will be a stack of parallel plates with an interferometer assembled between each pair of adjacent plates; the baseline length is 30 cm and the aperture is 5 cm. Figure 1 shows the optical plan for one of the interferometers.

Starlight from folding flats M_1 and M_1' in each interferometer combines at a 15 deg incidence angle at beamsplitter BS. A beam from each beamsplitter exit port is directed into a spectrometer. Each of Newcomb's 3 or 4 interferometers requires two of these spectrometers. The usual beam-compressing telescopes are absent, which reduces the number of components, the light loss in reflections, and beamwalk on M_1 and M_1'. The spectrometers employ prisms instead of gratings because of the light loss of the latter, which would be especially severe over the Newcomb optical passband (nominally 0.9 to 0.3 μm). The high loss would have contributions from the blazing, which could not be optimum over the whole passband, and from the filters needed to defeat the response at undesired grating orders. Finally, we have changed the beamsplitter incidence angle from 45 to 15 deg, both to simplify the design of the beamsplitter and to facilitate the thermal control of a compact design.

No comprehensive study has yet been made of systematic error in Newcomb. However, we know that the stability of the location of the elements M_1, M'_1, M_2, and BS is critical; the stability of the camera mirrors (M_4 and M'_4) and the detectors is also important. Although we initially planned to have no laser metrology, we now intend to make use of simple, null type, laser gauges. We plan to construct the instrument of solid ULE, which has an expansion coefficient 1×10^{-8}/K for small pieces of selected material. (In a worst case, we may assume that this varies by 100% across the instrument.) Thermal expansion of the 0.3 m dimensions must contribute no more than 30 μas to the instrument bias. Then the instrument average temperature and temperature gradients must be held constant to within ~0.015 K over the recalibration timescale of several hours. Our thermal studies of POINTS have shown that this level of control is likely to be achievable, even accounting for the variation in thermal input from the warm spacecraft, the Earth, and the Sun.

3. THE STAR-GRID PROBLEM

A fundamental issue for an astrometric instrument is the availability, characteristics, and selection of the reference stars. Once a target star is selected, the instrument must be able to observe a suitable set of reference stars. For POINTS, the reference stars are selected within a band between 87 and 93 deg from the target. This band covers 5% of the sky and contains numerous bright stars, *e.g.*, about 80 of $m_v \leq 5$.

For Newcomb, we wish to avoid the cost and complexity of a POINTS-like articulation and the associated system of laser gauges. Initially, we planned to have a channelled spectrum fall on a long detector array: 8k cells. This would yield a 21 arc min Nyquist angle for the 30 cm baseline. More recently, however, a detailed analysis of the Newcomb spectrometer has shown that because of the non-uniformity of dispersion, diffractive blur, and geometrical aberration, fringe visibility would fall to an unacceptably low level far short of 21 arc min. We have therefore revised the design. We now envision operating with three to seven fringes on a relatively short detector array. We will move the beamsplitter assembly (BSA) along the baseline direction to compensate the change of optical path difference associated with a target away from the nominal interferometer axis. With this design change, we are now free to increase

the aperture and baseline length, subject to evaluation of the effect on systematic error. The added complexity caused by allowing the beamsplitter assembly to translate has the compensating benefit of simplifying the spectrometer and detector.

There are several options for translating the beamsplitter assembly. The use of three "inchworms" is attractive. Two of these PZT motors would be placed at A in Fig. 1, one each near the "top" and the "bottom" of the optical paths. The third would be at B. These motors would provide ±2 mm displacement, corresponding to ±0.38 deg (±23 arc min) target direction deviation from the nominal interferometer axis. For a pair of interferometers, the combined deviations would yield pseudo-articulation limits of ±0.76 deg. A rotation of the beamsplitter assembly around the baseline direction makes a second-order contribution to the measured angle: $\varepsilon = Q\theta^2$, where ε is the interferometer angle error, θ is the rotation, and Q=1.1 μas/arcsec^2. To hold the error to 10 μas requires that the two sides of the BSA move parallel to within 2 μm.

A set of three laser gauges (with a single laser driving all gauges in all stellar interferometers) would monitor the motions of the three motors. These would operate in fringe counting mode during motor slew and as sensors for a null servo during starlight observations. The error signal from each laser gauge would be fed back to a fine position (PZT) actuator associated with the corresponding motor. This system would control the translation for the BSA and two degrees of its rotational freedom.

The mission concept for Newcomb relies on a reference grid of stars and a redundant set of intra-grid observations that permit the grid star positions to form a tightly connected system. This aspect of a Newcomb mission resembles a POINTS mission[2,3,4] for which the critical quantity is the redundancy factor:

$$M = \frac{\text{number of observations}}{\text{number of stars in the grid}} \qquad (1)$$

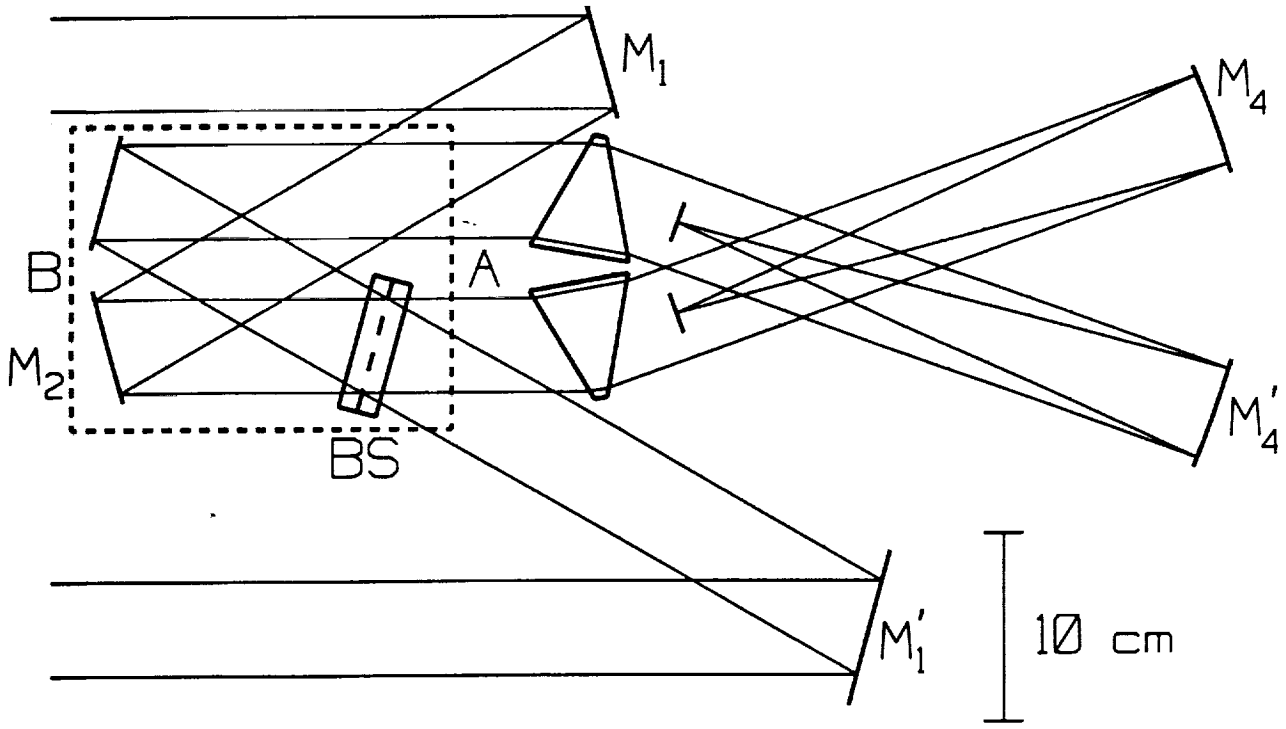

Figure 1. Optical plan for one Newcomb interferometer. All optics up to the spectrometer camera mirrors M_4 and M_4' are in one plane. M_4 and M_4' are off-axis paraboloids which deflect the beams out of the page, so that the detectors are above the beams that emerge from the prisms.

From our studies of POINTS, we know that when $M > M_0$, where M_0 is about 3.5, the grid "locks up" such that the angle between any pair of stars can be determined by the analysis of the data, even when the pair of interest cannot be directly observed. For POINTS, we normally assume M=5 in studies of the mission. In the nominal POINTS architecture, the angle between a pair of stars to be observed must be $\phi=\phi_o+\Delta$, $|\Delta| \le \Delta_o$, where ϕ_o=90 deg and Δ_o is the one sided articulation range (in degrees). If POINTS observes all of the star pairs within its articulation range, then

$$N^* = \frac{115\ M}{\Delta_O \sin\phi_o} \qquad (2)$$

where N^* is the number of stars in the grid. For POINTS, with the nominal parameters of M=5 and Δ_o=3 deg, we find that $N^* \approx 191$.

For Newcomb, if we were to have two interferometers at ϕ_o=90 deg, and if we assumed M=5 and Δ_o=0.76 deg, then we would find that $N^* \approx 750$. If the instrument can make D observations per day, the time needed to make a complete set of grid-star observations is $M \times N^*/D$. Since D is of order 200, it would require 19 days to complete one observation cycle of the grid. This is clearly not acceptable. Further, for a spacecraft in low Earth orbit, the scheduling of the interferometer observations is simplified by making ϕ_o smaller than 90 deg. However, this makes N^* larger.

3.1. A sparse and regular star grid

An alternative to the random grid of stars is a regular pattern of small regions or *berths* arranged on the celestial sphere in such a way that a large number of pairs of such berths are separated by a few special angles. Of course, a sufficient number of berths would need to each contain a suitable grid star. Such a "crystal on the sky" could be based on one of the semi-regular polyhedra. As the starting point, we selected one of the biggest of these, the truncated regular icosahedron (a.k.a. buckyball), which has 60 vertices, 90 sides, and 32 surfaces (12 pentagons plus 20 hexagons); all vertices are equivalent. Of the 59 angles from a given vertex to the other vertices, the following repeat four times: 40.91, 60.51, 70.77, and 78.60 deg, and their supplements 139.09. 119.49, 109.23, and 101.40 deg. No angle repeats more than four times. Observation angles near 90 deg provide maximum sky area in which to find target stars, but smaller observation angles were expected to be advantageous for solar-glare isolation. A measurement grid must meet three increasingly stringent requirements: (1) it must lock up when a complete set of data is analyzed, (2) it must remain locked up when biases are estimated, and (3) it must be robust against deleting a moderate fraction of the stars. A Newcomb star grid is then the set of stars of sufficient brightness, but no more than one per berth, that are found in the set of berths. Grids were tested using the POINTS simulation program[5]. In a typical simulation, all observable star pairs were measured each quarter year for 9 quarters. Stars within a cone of adjustable size near the Sun were not observed. Five star parameters (two positions, parallax, and two proper motions) were estimated, as well as a variable number of Fourier bias parameters for each observation angle. Star positions and proper motions were given a weak *a priori* estimate to break the overall rotational degeneracy, and all measurements were assumed to have 100 μas precision.

A simple measure of grid robustness is the distribution of $\log_{10}$(inter-star angle uncertainty) for all star pairs. We prefer the mean of this to be somewhat smaller than $\log_{10}$(single measurement uncertainty), and that the distribution have few if any outliers. A robust system was assembled by using three sets of 60 berths and two measurement angles, 40.91 and 60.51 deg. The second and third sets of berths are rotated by ± 20.82 deg from the first around an axis through the centers of opposing pentagonal faces, which provides about 300 interconnections among the three sets of 60 berths. (With the previous, smaller pseudo-articulation, there were only 40 interconnections.) The grid is robust against deletion of roughly one third of the stars, even if biases are estimated and near-Sun observations are excluded. With 120 stars in the grid, the statistical uncertainty of relative star position increased by only 31% due to degeneracy (*i.e.*, with constant number of observations.) With 90 stars, the grid is still stable, but the relative position uncertainty increases by a factor of 4.5.

3.2. Finding stars in the berths

In the preceding section, we were concerned with the star grid as an abstract construct. Here we address the characteristics of a star grid based on real stars. When we initially select specific stars to form a grid on the sky, we require that each grid star be within the deviation angle of the nominal position, *i.e.*, to require that each selected star be

within a circular berth with a radius equal to the deviation angle, and centered on the nominal position. For historical reasons, our studies have been done with a deviation angle of 21 arc min. For these studies, each grid star must be located within a small circle of area 0.38 sq. deg on the celestial sphere. In principle, we can improve on the star grid developed according to the above procedure. For the berths initially unfilled, we could search for a suitable grid star in a wider region, limited only by the maximum combined deviation of two interferometers and the actual locations of the grid stars against which the new star needs to be measured. Thus far, our studies have not included this extension of the star-selection algorithm, which we expect would fill more than half of the initially unfilled berths.

Table 1 gives the average density of stars on the sky as a function of visual magnitude[6] and, based on Poisson statistics, the expected number of occupied berths. Note that the actual star density is roughly a factor of two higher than tabulated near the galactic plane, and a factor of two lower near the galactic pole. From the table, we see that if stars were uniformly distributed, the grid stars would only have to be as faint as m=9.

To provide a more realistic assessment of the number of berths that could contain a suitable grid star, we performed a Monte Carlo study. We started with the ~ 380,000 stars of the Position and Proper Motion (PPM) Catalog[7]. PPM magnitudes are mostly photographic in the Northern hemisphere, mostly visual in the Southern. No correction was applied to the magnitudes. In our sensitivity studies, we use the bolometric magnitude and treat the signal as light from a black body of specified temperature passing through the optical bandpass of the instrument. The "bolometric correction" provides more margin than one at first expects by examining the magnitudes of the available stars and our limiting magnitude specifications. For each of a series of random orientations of the set of 180 berths, we determined how many of the berths would contain a star of acceptable brightness. We then produced a histogram of the star counts. The random orientation of the 180-berth set was based on the Eulerian angles ϕ, θ, ψ. We provided a uniform distribution from 0 to 360 deg for the rotations ϕ and ψ around the z and z′ axes, and a uniform distribution from -1 to 1 for $\cos(\theta)$, where θ is the inclination angle.[8]

In one study, we considered all stars with $m \leq 9$. A run of 5000 cases required under an hour on a '486 PC running at 33 MHz. Figure 2 shows the resulting distribution. Our expectation of 120 stars, based on Poisson statistics and the average density of $m \leq 9$ stars, was in some respects optimistic. The Monte Carlo generated distribution peaks at 110 stars. However, there are about 300 cases with 120 or more berths containing a suitable star. This type of study was repeated for mags 8 through 10 in .5 mag steps. The results of this study strongly suggest that satisfactory stellar grids with a sufficient number of occupied berths can be found when the grid stars are no fainter than mag 9. The next step would be to investigate some of the more attractive cases to determine how well the grid locks and how robust it is against solar glare angle exclusion. A preliminary analysis suggests that the extended algorithm could yield a grid with $m \leq 8.5$.

Table 1. Density of stars

m_{vis}	Stars per 0.38 sq. deg	Expected no. of occupied berths
5	0.015	2.7
6	0.046	8.1
7	0.13	22
8	0.38	57
9	1.1	120
10	3.1	172
11	8.4	180
12	22	180
13	56	180
14	138	180

3.3. Sky coverage

A multitude of small patches of sky are observable relative to the reference grid. To investigate this numerically, sections of the sky were covered with a 0.1×0.1 deg lattice and the number of references stars visible from the center of each lattice box was tabulated. We assumed a reference star at the center of each of the 180 berths. (Because of the symmetry of the 180-star grid, the study region needed only cover 36 deg of longitude and from the equator to one pole.) The results of this study are optimistic to the extent that a real grid would have fewer than 180 stars.

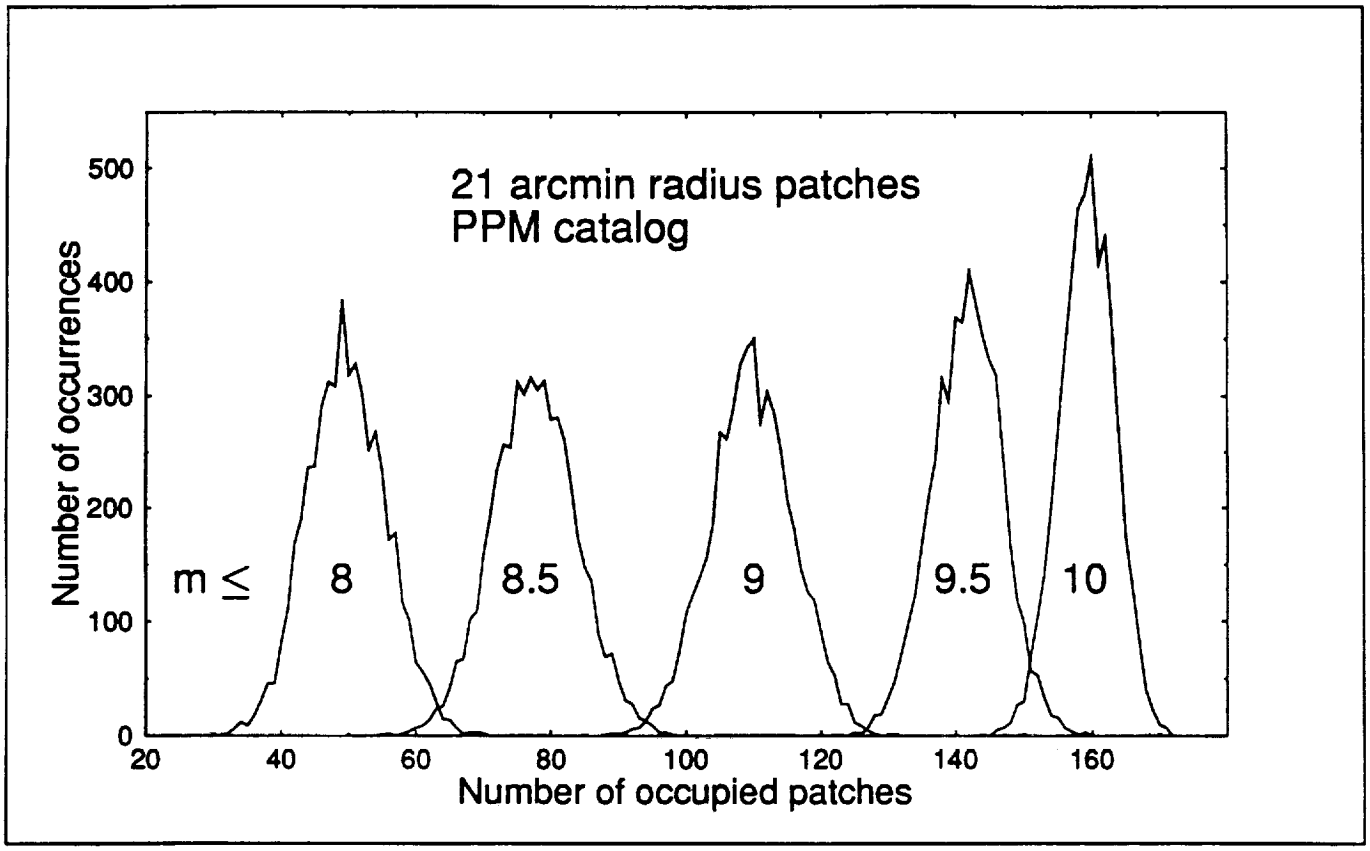

Figure 2. Distribution of the number of occupied berths for 5000 random grid orientations for limiting magnitudes of 8 to 10. A viable grid requires approximately 120 stars.

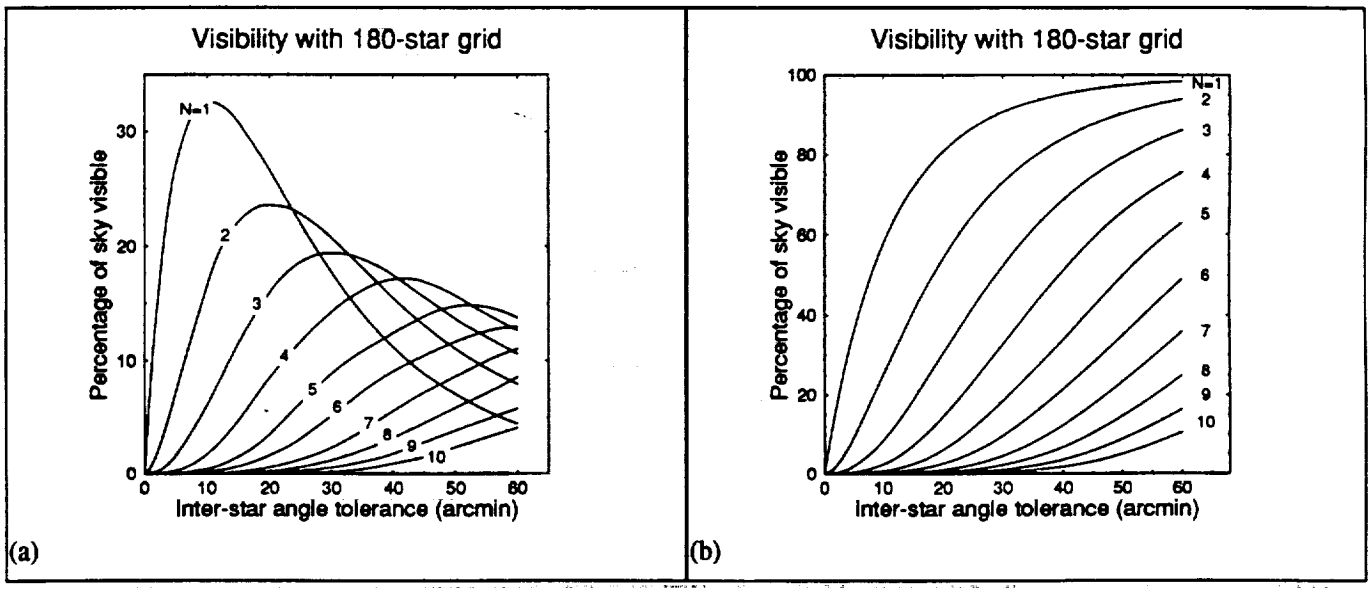

Figure 3. Fraction of sky observable against the 180-star Newcomb grid. The inter-star angle is 19.6, 40.91, or 60.51 deg, with a tolerance of ± 45 arcmin. Curves are labeled with N, (a) with exactly N reference stars and (b) with N or more reference stars. (Note that the 180 berths available for reference stars cover about (1/6)% of the sky.)

Figures 3a and 3b show the fraction of the sky visible against the nominal 180-star grid as a function of the inter-star angle tolerance. With a maximum deviation of 0.38 deg in each interferometer, about 75% of the sky can be observed with respect to at least the minimum of three references stars that are needed for a redundant position measurement, or to estimate star-specific biases. Additional coverage could be obtained with additional 60-star sub-grids. It might also be useful to put grid stars in the patches that neither contain nor lie near a grid star and that can be seen from at least six of the grid stars.

4. ACCURACY AND LIMITING MAGNITUDES

We have performed a preliminary investigation of the accuracy of the estimated star parameters that could be achieved during a nominal, 30 month mission. In the study, which was concerned only with the grid stars, we excluded measurements of stars less than 30 deg from the Sun. In the covariance studies, we assumed nine quarterly observation series and five bias parameters per series per observation angle. The nine quarterly observations series in a 30 month mission allows for some initial set up after launch. We found that the typical uncertainties for star relative position, relative annual proper motion, and absolute parallax are 29, 40, and 21 μas, respectively. In a second study, we assumed that 60 of the 180 possible stars would not be present. Since the star deletion process is stochastic, we repeated the study ten times. We found the ranges of the typical uncertainties to be 41.2-44.0, 56.8-61.2, and 26.7-27.9 μas, respectively. It will be seen in Section 5 that this is the correct level for several of the science objectives.

Two noise sources contribute to setting the limiting magnitude: (a) CCD effective dark current, which is due to read noise, and (b) sky background. The variance of the CCD read noise is N_r^2, where N_r, the rms number of noise electrons due to reading one pixel, is taken to be 3. To estimate the limiting magnitude due to read noise variance, we equate this to the variance of starlight, which is the average number of detected photons in a pixel, $\dot{N}_t \tau / P$, where $\dot{N}_t$ is the average photon detection rate in one beamsplitter exit port, *i.e.*, the detection rate corresponding to the photons collected by one folding flat; τ is the duration of one integration; and P is the number of filter pixels. Table 2 gives the limiting magnitudes for bright and faint stars. The faint star integration time, 5 min, is set by the cosmic ray rate in high Earth orbit. In the low orbit planned, the integration time could be longer, probably by as much as a factor of ten.

Sky background is mostly from faint Galactic stars and zodiacal light. The contributing patch of sky is much elongated in the dispersion direction. In the cross-dispersion direction, at λ=0.5 μm, the full width of a stripe of the detector containing 75% of the intensity corresponds to ≈9 arcsec on the sky. In the dispersion direction, with two stops of radius 5.1 cm separated by 1 m, the length of an equivalent rectangular stripe of sky is 2.5 deg. Taking a median sky brightness to be magnitude 21.8 per arcsec^2, the limiting magnitude is 9.5. This limit applies for both the bright and faint star interferometers. If a slit is added to the spectrometer, the sky background becomes much fainter: the acceptance angle in the dispersion direction drops by three orders from 2.5 deg to 7 arcsec.

5. APPLICATIONS

Newcomb would establish a precise reference frame that would be accessible to optical and infrared sensors. This frame would be useful to the Navy for navigation. The HIPPARCOS data already received will yield a grid that is good for a short time, but proper motion uncertainty from this short-duration mission will quickly degrade that grid. Newcomb and HIPPARCOS would complement each other for determining proper motion. Repeated and redundant observations would insure that the program was robust. Newcomb will also provide a direct link between high-precision optical astrometry and the present radio reference frame as discussed by Fey *et al.*,[9,10] and in the papers they cite. Observations of only a few radio quasars are needed to fix the relative rotation between the current radio reference frame and the optical reference frame that will be developed by Newcomb and HIPPARCOS. Newcomb will thus resolve current difficulties in relating high angular resolution observations at radio and optical wavelengths.

Newcomb could see enough of the sky to do some interesting science. If the spectrometer design includes a slit, the instrument's limiting magnitude would be about 15. However, the above analysis depends on instrument parameters that are not yet fixed and are expected to be set during a series of trade studies. The Space Interferometry Science

Working Group (SISWG) developed a Strawman Science Program for the Astrometric Interferometry Mission[11] as a step toward evaluating the astrophysical capability of the two candidate missions: POINTS and OSI. Of the goals presented in the "Strawman," five could also be addressed by Newcomb: (1) 19 known Cepheids have parallaxes between 200 and 1000 μas and m_v less than 10; a 5% distance measurement would be useful for refining the cosmic distance scale. (2) Absolute magnitudes of O stars are uncertain because none is close enough to allow a trigonometric parallax measurement from the ground. O stars are bright targets, m_v=4 to 6 at 1 to 2 kpc; 25 to 50 μas parallax measurements are needed. (3) Estimates of the ages of globular clusters often exceed estimates of the age of the universe. Age determinations of globular clusters depend in part on the calibration of the absolute magnitude of RR Lyrae stars as a function of period. The 20 brightest RR Lyrae stars range from m_v=7.6 to 10. Parallax measurements are needed at the 1% level, which corresponds to 40 μas for RR Lyrae itself. (4) Distances to 90 nearby field subdwarfs cataloged by Carney,[12] ranging in magnitude from 7.2 to 12, would calibrate subdwarf luminosities, which are used in fitting the globular cluster main sequences. Parallaxes are needed with 30 μas precision. (5) Parallaxes of bright (m_v=10) K giants in the galactic disk, accurate to 50 μas, would probe the dark matter in our Galaxy.

With 100 μas measurements and a sufficient mission duration, Newcomb could detect Jupiter-sized planets around nearby stars. The problem here is that, if the solar system is a "typical" planetary system, signatures large enough to be seen will have periods much longer than the 30 month life envisioned for Newcomb. HIPPARCOS measurements might help break the degeneracy between proper motion and a short arc of orbital motion, but this speculation has not yet been tested by a sensitivity study. Similarly, Newcomb data could supplement a POINTS mission, especially if the Newcomb mission significantly precedes the POINTS launch and in the case of a planet period that is long compared to the POINTS mission life, possibly shortened by equipment failure.

Table 2. Limiting magnitudes.

Symbol	Definition	Bright star value	Faint star value
τ (note a)	Integration time	0.1 sec	5 min
P (note b)	Number of filter pixels	20	1024
	Magnitude limitation from read noise	10.4	14.9
	Magnitude limitation from sky background (slitless spectrometer)	9.5	
	Magnitude limitation from sky background (with slit in spectrometer)	17.4	
	Instrument limiting magnitude (slitless spectrometer)	9.2	9.5
	Instrument limiting magnitude (with slit in spectrometer)	10.4	14.9

[a] The interferometer looking at the "bright star" provides the error signal to the fine pointing system. To have a unit gain frequency of 1 Hz, we require a 10 Hz sample rate. With the instrument thus stabilized, we are free to integrate for an extended period on the faint star. On some time scale, cosmic ray hits invalidate the data. The integration time for the faint star is set to keep such invalidation events rare. At a slight penalty in lost observing time, the integration time could be extended and the faint-star limiting magnitudes increased.

[b] The effective number of pixels is varied by co-adding the photo-electrons on the chip before reading the total detected charge. The co-adding process is nearly noiseless and nearly 100% efficient.

Gravity Probe B, an experiment which will measure the general relativistic frame dragging due to the spinning Earth, needs a bright guide star (Rigel) with proper motion known in an inertial frame to ~1 mas/year or better[13]. The proper motion of Rigel could be determined by Newcomb in its reference frame, which would be tied directly to a few bright quasars.

6. ACKNOWLEDGEMENTS

This work was supported in part by the NASA Planetary Instrumentation Definition and Development Program (PIDDP) Grant NAGW-2497, by NRL research contract # N00014-93-K-2036, and by the Smithsonian Institution. The authors gratefully acknowledge the careful preparation of the camera-ready text by S.A. Silas.

7. REFERENCES

1. R.D. Reasenberg, R.W. Babcock, J.D. Phillips, K. Johnston, and R. Simon, "Newcomb, a POINTS precursor mission with scientific capacity," The Proceedings of the SPIE Conference # 1947 on Spaceborne Interferometry, (Orlando, FL, April 14-16, 1993), Vol. 1947, pp. 272-281, 1993.

2. R.D. Reasenberg, R.W. Babcock, M.C. Noecker, and J.D. Phillips, "Space-based astrometric optical interferometry with POINTS," The Proceedings of the ESA Colloquium on Targets for Space-Based Interferometry, European Space Agency, Beaulieu-sur-Mer, France, 13-16 October 1992, ESA Publications Division, Noordwijk, The Netherlands, ESA-SP-345, pp. 59-69, December 1992.

3. R.D. Reasenberg, R.W. Babcock, M.C. Noecker, and J.D. Phillips, "POINTS: The Precision Optical INTerferometer in Space, in Remote Sensing Reviews (Special Issue Highlighting the Innovative Research Program of NASA/OSS), Guest Editor: Joseph Alexander, 1993.

4. R.D. Reasenberg, "Microarcsecond Astrometric Interferometry," in Proceedings of IAU Symposium, 109, Astrometric Techniques (Gainesville, 9-12 January 1984), H.K. Eichhorn and R.J. Leacock, eds. pp. 321-330, Reidel, Dordrecht, 1986.

5. J.F. Chandler, and R.D. Reasenberg, "POINTS: A Global Reference Frame Opportunity," Inertial Coordinate System on the Sky, J.H. Lieske and V.I. Abalakin, Eds. Kluwer Academic Publisher, Dordrecht, pp. 217-227, S. 141, 1990.

6. C.W. Allan, Astrophysical Quantities, The Athlone Press, p. 244, London, 1976.

7. S. Rösner, and U. Bastian, Astron. Astrophys. Suppl. Ser., 74, 449-451, 1988.

8. H. Goldstein, Classical Mechanics, The A-W Series in Advanced Physics, p. 107, Addison Wesley, Reading Massachusetts, 1959.

9. A. Fey, J.L. Russell, C. Ma, K.J. Johnston, B.A. Archinal, M.S. Carter, E. Holdenreid, and Z. Yao, Astron. J. 104, 891, 1992.

10. A. Fey, J.L. Russell, C. de Vegt, N. Zacharias, K.J. Johnston, C. Ma, D.M. Hall, and E.R. Holdenreid, Astron. J., 107, p. 385 (Paper VI), 1994.

11. "Astrometric Interferometry Mission Strawman Science Program," Space Interferometry Science Working Group [established by the Astrophysical Division of NASA and chaired by S. Ridgway], 5 July 1992.

12. B.W. Carney, "The Subdwarf Helium Abundance and the Rotation of the Galactic Halo," Astrophys. J., 233, p. 877, 1979.

13. C.W.F. Everitt, D.E. Davidson, R.A. Van Patten, "Cryogenic star-tracking telescope for Gravity Probe B," The Proceedings of SPIE Conference # 619 Cryogenic Optical Systems and Instruments II, Vol. 619, pp. 89-119, 1989.